Author/s:
Fryer, AL;Abdullah, A;Mobilio, F;Jobling, A;Moore, Z;de Veer, M;Zheng, G;Wong, BX;Taylor, JM;Crack, PJ

Title:
Pharmacological inhibition of STING reduces neuroinflammation-mediated damage post-traumatic brain injury

Date:
2024-09-01

Citation:
Fryer, A. L., Abdullah, A., Mobilio, F., Jobling, A., Moore, Z., de Veer, M., Zheng, G., Wong, B. X., Taylor, J. M. & Crack, P. J. (2024). Pharmacological inhibition of STING reduces neuroinflammation-mediated damage post-traumatic brain injury. British Journal of Pharmacology, 181 (17), pp.3118-3135. https://doi.org/10.1111/bph.16347.

Persistent Link:
https://hdl.handle.net/11343/351312

Received: 4 August 2023 | Revised: 4 January 2024 | Accepted: 16 January 2024

DOI: 10.1111/bph.16347

RESEARCH ARTICLE

Pharmacological inhibition of STING reduces neuroinflammation-mediated damage post-traumatic brain injury

Amelia L. Fryer[1] | Amar Abdullah[1,2] | Frank Mobilio[1] | Andrew Jobling[3] | Zachery Moore[1,4,5] | Michael de Veer[6] | Gang Zheng[6] | Bruce X. Wong[1] | Juliet M. Taylor[1] | Peter J. Crack[1]

[1]Neuropharmacology Laboratory, Department of Biochemistry and Pharmacology, University of Melbourne, Parkville, Australia

[2]Department of Biological Sciences, School of Medical and Life Sciences, Sunway University, Subang Jaya, Malaysia

[3]Department of Anatomy and Physiology, University of Melbourne, Parkville, Australia

[4]Personalised Oncology Division, The Walter and Eliza Hall Institute of Medical Research, Melbourne, Australia

[5]Department of Medical Biology, University of Melbourne, Parkville, Australia

[6]Monash Biomedical Imaging, Monash University, Clayton, Australia

Correspondence
Peter Crack, Neuropharmacology Laboratory, Department of Biochemistry and Pharmacology, University of Melbourne, Parkville 3010, Australia.
Email: pcrack@unimelb.edu.au

Funding information
National Health and Medical Research Council (NHMRC), Grant/Award Number: 1156744; The Brain Foundation

Background and Purpose: Traumatic brain injury (TBI) remains a major public health concern worldwide with unmet effective treatment. Stimulator of interferon genes (STING) and its downstream type-I interferon (IFN) signalling are now appreciated to be involved in TBI pathogenesis. Compelling evidence have shown that STING and type-I IFNs are key in mediating the detrimental neuroinflammatory response after TBI. Therefore, pharmacological inhibition of STING presents a viable therapeutic opportunity in combating the detrimental neuroinflammatory response after TBI.

Experimental Approach: This study investigated the neuroprotective effects of the small-molecule STING inhibitor n-(4-iodophenyl)-5-nitrofuran-2-carboxamide (C-176) in the controlled cortical impact mouse model of TBI in 10- to 12-week-old male mice. Thirty minutes post-controlled cortical impact surgery, a single 750-nmol dose of C-176 or saline (vehicle) was administered intravenously. Analysis was conducted 2 h and 24 h post-TBI.

Key Results: Mice administered C-176 had significantly smaller cortical lesion area when compared to vehicle-treated mice 24 h post-TBI. Quantitative temporal gait analysis conducted using DigiGait™ showed C-176 administration attenuated TBI-induced impairments in gait symmetry, stride frequency and forelimb stance width. C-176-treated mice displayed a significant reduction in striatal gene expression of pro-inflammatory cytokines *Tnf-α*, *Il-1β* and *Cxcl10* compared to their vehicle-treated counterparts 2 h post-TBI.

Conclusion and Implications: This study demonstrates the neuroprotective activity of C-176 in ameliorating acute neuroinflammation and preventing white matter neurodegeneration post-TBI. This study highlights the therapeutic potential of

Abbreviations: c-di-GMP, bis-(3′-5′)-cyclic dimeric guanosine monophosphate; C-176, n-(4-iodophenyl)-5-nitrofuran-2-carboxamide; DAMP, danger-associated molecular pattern; IRF3, interferon regulatory factor 3; TBI, traumatic brain injury.

Amelia L. Fryer and Amar Abdullah contributed equally to this work. Juliet M. Taylor and Peter J. Crack contributed equally to this work.

small-molecule inhibitors targeting STING for the treatment of trauma-induced inflammation and neuroprotective potential.

KEYWORDS
neurodegeneration, neuroinflammation, STING, traumatic brain injury

1 | INTRODUCTION

Traumatic brain injury (TBI) is a leading cause of death and disability in industrialised nations (Dewan et al., 2019). TBI is a multifaceted pathology that varies in severity from a mild concussion to severe injury resulting in coma or death. Lasting neurobehavioral effects differ with severity of TBI and include attention deficits, poor cognition, development of anxiety or depression, antisocial behaviour, severe fatigue and sleep disturbances (Alosco et al., 2020; Vaughn et al., 2019). Current medical interventions for TBI primarily stabilise the patient while there is no therapeutic intervention available after patient stabilisation, resulting in a severe unmet need for new medical interventions targeting deleterious secondary injury cascades and conferring neuroprotection (Cook et al., 2020; Khellaf et al., 2019). Secondary injury in TBI is a complex array of interrelated molecular processes, such as excitotoxicity, necrosis and neuroinflammation, which all contribute to chronic neurodegeneration (Dixon, 2017; McConeghy et al., 2012). This chronic neurodegeneration is implicated in the worsening of neurological function that is observed following TBI (Loane et al., 2014). Targeting secondary injury presents therapeutic potential to minimise progressive neuronal cell death and improve motor and cognitive outlook.

A key mediator implicated in the chronic neurodegeneration and worsened neurological function associated with secondary injury is neuroinflammation (Karve et al., 2016; Loane et al., 2014; Simon et al., 2017). The initial neuroinflammatory response following TBI is chiefly driven in response to the abundant cell death and BBB disruption that occurs as a result of the primary injury (Corps et al., 2015). Dysregulated neuroinflammation can prevail for weeks to years following TBI (Johnson et al., 2013). This persistent neuroinflammation is strongly linked to the chronic neurodegeneration seen in TBI as well as a host of neurodegenerative conditions including stroke, Alzheimer's disease and Parkinson's disease (Lee et al., 2019; Minter et al., 2016; Zhang et al., 2017). Damage-associated molecular patterns (DAMPs) released by dying cells following TBI can result in the rapid release of pro-inflammatory molecules by microglia and astrocytes. These molecules include pro-inflammatory cytokines and chemokines such as **type-I interferons (IFNs)**, **tumour necrosis factor alpha (TNFα)** and **interleukin 1 beta (IL-1β)** (Karve et al., 2016; Knoblach et al., 1999).

A critical pro-inflammatory mediator released by microglia and astrocytes to drive neuroinflammation are the type-I IFNs. Type-I IFNs are pleiotropic cytokines that have been implicated in the exacerbation of neuroinflammation following TBI and in the neurodegeneration observed in a host of other neurological disorders such as Aicardi-Goutiers syndrome (AGS), Alzheimer's disease and systemic lupus erythematosus (SLE) (Barrett et al., 2020; Crow et al., 2006; Karve et al., 2016; Minter et al., 2016). **Stimulator of interferon Genes (STING)**, also known as transmembrane protein 173 (TMEM173), endoplasmic reticulum interferon stimulator (ERIS) and mediator of interferon regulatory factor 3 activation (MITA), is an endoplasmic reticulum (ER) bound transmembrane adaptor protein (Ishikawa & Barber, 2008). It plays a critical role in up-regulating type-I IFN expression through the cGAS-STING pathway upon detection of cytosolic double-stranded DNA (dsDNA) (Ishikawa et al., 2009; Tanaka & Chen, 2012).

dsDNA is recognised as a DAMP by the enzyme **cyclic GMP-AMP synthase (cGAS)**, which initiates downstream signalling through STING, up-regulating type-I IFN production (Chen et al., 2016; Sun et al., 2013). Once bound to dsDNA, cGAS facilitates the production of a cyclic dinucleotide, **2′3′-cyclic adenosine monophosphate guanosine monophosphate (2′3′-cGAMP)** from **adenosine triphosphate (ATP)** and **guanosine triphosphate (GTP)** (Ablasser et al., 2013). 2′3′-cGAMP is the endogenous agonist of STING that induces STING oligomerisation (Ablasser et al., 2013;

What is already known

- Dysregulated neuroinflammation is a key driver of secondary injury in traumatic brain injury (TBI).
- Genetic deletion of stimulator of interferon genes (STING) is neuroprotective against TBI-induced inflammation in mice.

What does this study add

- Administration of STING-inhibitor C-176 post-TBI ameliorates cortical damage, neuroinflammation and improves neurobehavioural outcomes.

What is the clinical significance

- Targeting the cGAS-STING pathway with small-molecule inhibitors minimises secondary injury post-TBI and displays neuroprotection.

Shang et al., 2019). The activated STING oligomer translocates to the Golgi apparatus, where it recruits and phosphorylates kinases **TANK binding kinase 1 (TBK1)** and **IκB kinase (IKK)** forming multimeric dimers at the cytosolic domain of STING (Zhang et al., 2019). Activated STING, TBK1 and IKK recruit and phosphorylate interferon regulatory factor 3 (IRF3) and nuclear factor kappa-light-chain-enhancer of activated B cells (NF-κB) at the C-terminal tail of STING (Tanaka & Chen, 2012). IRF3 and NF-κB are both promoters of type-I IFN transcription and once activated, they migrate to the nucleus, bind to IFN promoter regions and potently up-regulate type-I IFN production (Ishikawa & Barber, 2008). Following activation, STING is rapidly degraded by lysosomes (Gonugunta et al., 2017).

Aberrant STING activity is increasingly being recognised to be damaging in contexts of acute and chronic sterile inflammation in neurodegenerative pathologies including stroke, Parkinson's disease, Huntington's disease, amyotrophic lateral sclerosis, ageing and TBI (Barrett et al., 2020; Peng et al., 2020; Sliter et al., 2018; Yu et al., 2020). Our group have previously established genetic deletion of STING signalling to be neuroprotective in the controlled cortical impact mouse model of TBI with *Sting*$^{-/-}$ mice displaying significantly smaller lesion size 24 h post-TBI compared to wildtype mice (Abdullah et al., 2018). Work conducted by Sen et al. (2020) found that indirectly inhibiting STING signalling through the ER-stress sensor **protein kinase R-like ER kinase/eukaryotic translation initiation factor 2 alpha kinase 3 (PERK)** elicited similar neuroprotective outcomes in the controlled cortical impact TBI mouse model. Furthermore, use of a STING agonist has been shown to exacerbate behavioural changes and pyroptosis in a rodent model of severe TBI (Zhang et al., 2022), further suggesting that attenuating STING-mediated inflammation post-TBI is neuroprotective in mice.

As a targetable upstream modulator of type-I IFN signalling, the discovery of STING has generated new excitement in therapeutically harnessing inflammation (Sheridan, 2019). Unlike **interferon α/β receptor (INFAR) 1** and **2**, STING is readily targetable using small-molecule agonists and antagonists, offering a new opportunity to therapeutically modulate type-I IFN production (Feng et al., 2020; Fu et al., 2015; Haag et al., 2018). Small-molecule nitrofuran derivative compounds have been found to inhibit STING activity by blocking activation-induced palmitoylation, which renders STING unable to form complexes in the Golgi apparatus in response to cyclic dinucleotide binding (Haag et al., 2018; Hansen et al., 2018). Use of these small molecule inhibitors in mouse models of amyotrophic lateral sclerosis (ALS), subarachnoid haemorrhage (SAH) and severe TBI has observed neuroprotective effects, with mice displaying improvements in behaviour testing and a reduction in expression of pro-inflammatory cytokines and attenuated neuronal injury (Peng et al., 2020; Yu et al., 2020; Zhang et al., 2022).

In this study, we employed the controlled cortical impact model of mild TBI to evaluate the use of a small-molecule STING inhibitor (**C-176**) to confer neuroprotection post-mild TBI. Our group has previously confirmed that genetic deletion of STING in this mouse model was successful in reducing the lesion size. We hypothesise that small-molecule inhibition of STING will be protective against STING-mediated neuroinflammation. Here, we report that administration of C-176 in a post-controlled cortical impact modelled TBI is neuroprotective by reducing white matter neurodegeneration around the lesion area and improving neurobehavioral outcomes.

2 | METHODS

2.1 | Cell culture

BV2 cells were cultured in Dulbecco's modified eagle medium (DMEM) (Gibco, Cat. No. 11995-065) containing 5% foetal bovine serum (FBS) (Interpath, Cat. No. SFBSNZ5) and 1% penicillin–streptomycin (Life Technologies, Cat. No. 15070063) at 37°C/5% CO_2. Cells were plated in a six-well plate at a density of 1×10^6 cells per well. Cells were pre-treated for 30 min in media containing 0.1- to 2-μM C-176 or a DMSO vehicle. Following pre-treatment, cyclic di-GMP (c-di-GMP) (Invivogen, Cat. No. tlrl-nacdg) was added to a final well concentration of 10–20 $\mu g \cdot ml^{-1}$ for 8 h. Control wells were treated with an equivalent volume of endotoxin-free water. Following treatments, culture medium was removed and wells were gently rinsed twice with ice cold phosphate-buffered saline (PBS) (Life Technologies, Cat. No. 18912014). Cells were scraped in PBS using a hand-held cell scraper and placed in a cold Eppendorf tube. Samples were centrifuged at 3000*g* at 4°C for 10 min. Supernatants were removed and cell pellets stored at −80°C until required.

2.2 | Animals

All animal experiments were carried out on adult male C57BL/6J mice or male and female CXCR1^{EGFP} mice aged 8–12 weeks old with an average body weight of 23 ± 3 g. C57BL/6J mice were sourced from the Animal Resources Centre (Western Australia) and CXCR1^{EGFP} were a gift from Dr Andrew Jobling (University of Melbourne). Mice were housed in groups of up to five per micro-isolator cage on a 12:12 h light/dark cycle, with irradiated rodent chow and water provided *ad libitum*. All procedures, monitoring and reporting were performed in accordance with standard protocols approved by the University of Melbourne Animal Ethics Committee (Ethics ID # 1814589.4). Animal studies are also reported in compliance with the ARRIVE guidelines (Percie du Sert et al., 2020) and with the recommendations made by the British Journal of Pharmacology (Lilley et al., 2020).

2.2.1 | Experimental groups

Mice were randomly assigned to receive either a sham or mild controlled cortical impact surgery (TBI). Thirty minutes following impact, a 200-μL intravenous tail vein injection of 750-nmol C-176 diluted in phosphate-buffered saline (PBS) or a PBS vehicle was administered. Blinding of both the operator and data analysis was conducted by concealing the identity of the solution administered to mice post-TBI.

Magnetic resonance imaging (MRI) measuring lesion size was performed 24 h and 7 days after TBI. DigiGait™ analysis measuring behavioural outcome was conducted 24 h after TBI and biochemical analysis was conducted 2 h and 24 h after TBI. In this study, the identity of each animal with respect to treatment was blinded to researchers who conducted the experiments and analysis.

2.3 | Controlled cortical impact

The controlled cortical impact (CCI) procedure performed in this study was based on standard protocols as previously described and reported by our group (Karve et al., 2016). This model of TBI was selected as it is well documented to model secondary-injury inflammatory processes in addition to its high degree of reproducibility (Osier & Dixon, 2016). Mice were anaesthetised with ketamine (100 $mg{\cdot}kg^{-1}$)/xylazine (10 $mg{\cdot}kg^{-1}$) via intra-peritoneal injection. Mice were placed on a covered heat mat to maintain body temperature, respiratory rate was closely monitored and ocular lubricant was routinely applied to prevent corneal desiccation. A sagittal incision was made to expose the skull before a 2-mm diameter craniotomy was performed using a handheld electrical drill (Dremel, 10.8 V) at 2.5 mm lateral the midline and 1.5 mm posterior to the bregma to expose the right parietal cortex. The mice were placed in a stereotaxic frame for the injury to be delivered using a 2-mm flat computer-controlled impactor (LinMot-Talk 1100). An impact 1.5 mm deep was applied to the exposed cortex at a velocity of 1 $m{\cdot}s^{-1}$ and a dwell time of 100 ms. The skull flap previously removed during the craniometry was replaced over the exposed cortex and the sagittal incision was sutured by hand using wax coated braided silk. Thirty minutes following successful controlled cortical impact, mice were administered either C-176 or PBS intravenously. Post-surgery, all mice were administered buprenorphine (0.6 $mg{\cdot}kg^{-1}$) intraperitonially and placed on a heat mat to recover from anaesthesia, and their condition was monitored hourly over 6 h and the subsequent morning. Sham mice underwent identical anaesthesia, sagittal incision and craniometry as TBI mice, omitting the impact by the computer-controlled impactor. The mice were housed for 2 h or 24 h following surgery and killed by cervical dislocation before subsequent analysis.

2.4 | MRI acquisition

MRI scans were performed for this study using a Bruker 9.4 Tesla small animal MRI scanner (Monash Biomedical Imaging) to quantify the progression of tissue damage. Mice were anaesthetised with ~3% isoflurane in a 1:1 mixture of medical-grade air and oxygen. Anaesthesia was maintained throughout scanning with 0.25% to 1.5% isoflurane through a nosecone placed over the animal's snout and respiration was continuously monitored throughout the experiment with a pressure-sensitive probe positioned under the animal's diaphragm. Anaesthetised animals were laid supine on a purpose-built small-animal holder and their heads fixed into position with ear and bite bars. A surface receiver coil was placed over the animal head and the cradle was inserted into a transmitter coil fixed inside a BGA12S-HP gradient set for imaging. The MRI protocol consisted of a three-plane localiser sequence followed by multiecho T2 and diffusion-weighted sequences. The total scanning time was kept to <1 h per animal. Multiecho T2-weighted images were acquired using a rapid acquisition, relaxation enhanced (RARE) sequence with RARE factor = 2; repetition time = 2500 ms; effective echo time (TEeff) = 10, 30, 50, 70, 90 and 110 ms; field-of-view = 1.6 Å ~ 1.6 cm^2; matrix = 192 Å ~ 192; and 24 slices with thickness = 0.5 mm. Volumetric analysis was carried out on T2-weighted images using MRIcroGL software, available from www.nitrc.org/projects/mricrogl (Rorden & Brett, 2000).

2.5 | Gait analysis

The gait dynamics of the mice pre-and post-surgery were recorded non-invasively using a DigiGait™ apparatus (v11.5, Mouse Specifics™, MA, USA). The apparatus consists of a transparent conveyor belt over a recording device to capture the gait dynamics of the mice from underneath the belt. The belt was set to operate at a fixed speed of 15 $cm{\cdot}s^{-1}$ at an incline of 0°. Light fur and tails were coloured with black ink to reduce noise in recording. Mice were given one 'test run' prior to recording. The gait dynamics of the mice were recorded in triplicate over a running period of 4 s for each recording. Gait indices were quantified using the DigiGait™ Imaging System. The duration of each gait interval, which includes the duration of the stride, stance, swing, braking and propulsion phase (seconds), was used for gait analysis (Table 1).

2.6 | Western blot analysis

2.6.1 | Protein isolation

Protein extraction from cells was conducted using radioimmunoprecipitation assay (RIPA) lysis buffer comprising of 50-mM tris-HCL, 150-mM NaCl, 1% Triton X-100, 0.1% sodium dodecyl sulphate (SDS), 0.5% sodium deoxycholate, 2-mM ethylenediaminetetraacetic acid (EDTA), half of a cOmplete™ protease inhibitor cocktail tablet and one PhosSTOP™ phosphatase inhibitor cocktail tablet. Fifty microlitres of buffer was added to each cell pellet, samples were sonicated for 10 pulses at 10% followed by incubation on ice for 30 min before storage at −80°C.

Mouse brains were dissected into ipsilateral and contralateral hemispheres, and the cortex and striatal regions were isolated from each hemisphere. Samples were snap-frozen in liquid nitrogen and finely ground using a mortar and pestle. The ground sample was then further mechanically homogenised using a silicon microtube pestle at a tissue weight to homogenisation buffer ratio of 1:4. The homogenisation buffer comprised of 10% tris-buffer (50 mM tris-hydrochloride and 150-mM sodium chloride), 1% triton x-100, one cOmplete™ protease inhibitor cocktail tablet and half of a PhosSTOP™ phosphatase inhibitor cocktail tablet. The homogenised samples were placed on a microtube roller for

TABLE 1 Definition of DigiGait parameters.

Gait parameter	Definition	Unit of measurement	Use in mouse models of traumatic brain injury (TBI) or spinal cord injury (SCI)
Swing duration	Time duration of the paw is off the treadmill (swing phase).	Seconds (s)	Ek et al. (2010); Neumann et al. (2009); Sashindranath et al. (2015)
Stance duration	Duration of paw contact with treadmill (stance phase)	Seconds (s)	Neumann et al. (2009); Sashindranath et al. (2015)
Stride duration	Time taken to complete one stride	Seconds (s)	Neumann et al. (2009); Sashindranath et al. (2015)
Stride frequency	The number of strides a paw completes each second. Also known as 'cadence'.	Strides per second	Krizsan-Agbas et al. (2014); Sashindranath et al. (2015)
Stance width	The width between the forelimb and hindlimbs at peak stance. Also referred to as 'base of support'.	cm	Ek et al. (2010); Krizsan-Agbas et al. (2014)
Gait symmetry	Ratio of forelimb stepping frequency to hind limb stepping frequency. A metric for coordination. Healthy mice should have a ratio close to one.	Real #	Krizsan-Agbas et al. (2014)

2 h at 4°C before centrifugation at 2000*g* for 10 min. Supernatants were placed in fresh tubes and stored at −80°C for protein analysis. All Immuno-related procedures used comply with the recommendations made by the *British Journal of Pharmacology* (Alexander et al., 2018).

2.6.2 | Western blot

Protein concentration was determined by Bradford assay. Isolated proteins were incubated with 2× Novex™ tris-glycine SDS sample buffer (Thermo, Cat. No. LC2676) containing 5% 2-mercaptoethanol for 5 min at 90°C. Twenty to forty micrograms of protein was resolved on 10% acrylamide SDS-0 (PAGE) gels. Gels were transferred to polyvinylidene fluoride (PVDF) membranes using a Trans-Blot® SD semi-dry transfer cell (Bio-Rad, Cat. No. 1703940). Membranes were then blocked in 5% w/v skim milk in tris-buffered saline (TBS) with 0.05% Tween-20 (TBS-T) for 1 h, followed by an overnight incubation at 4°C with primary antibody (Table S1, Data S1) diluted in 5% w/v skim milk. The membranes were washed three times for 10 min each with TBS-T and incubated with horseradish peroxidase (HRP) conjugated secondary antibody (Table S2) in 5% w/v skim milk for 1 h at room temperature. Membranes were washed again with TBS-T and signals detected using an Amersham™ ECL™ prime western blotting detection kit (GE Healthcare, Cat. No. GEHERPN2232) and imaged using a ChemiDoc™ imaging XRS+ system (Bio-Rad, Cat. No. 1708265). Band intensity was measured using Image Lab™ software (Bio-Rad, Version 6.0.1) and normalised to the β-actin loading control. Values are presented as band intensity relative to β-actin.

2.7 | Quantitative real-time PCR

2.7.1 | RNA isolation

Brains were dissected into ipsilateral and contralateral hemispheres and cortex and striatal regions isolated from each hemisphere 24 h after TBI and sham surgery. The samples were snap frozen in liquid nitrogen and mechanically ground. Samples were mechanically homogenised in 1-ml TRIzol™ using a 21″ gauge needle. One-part degassed chloroform was added to 5 parts sample in TRIzol™ solution,and samples were spun at 12,000*g* for 15 min. The aqueous layer was removed and transferred to filter columns from an Illustra™ RNAspin mini isolation kit (GE Healthcare, Cat. No. 25050071). Further purification and DNase treatment of the RNA was conducted as per kit instructions. RNA was eluted in 50-µl RNase-free H_2O and the eluate re-applied to the spin column again and re-spun. Concentration and purity (260/280 nm and 260/230 nm) of RNA was measured using a NanoDrop 1000 spectrophotometer.

2.7.2 | qPCR

cDNA was diluted 1:10 with RNase-free water. The TaqMan or SYBR Green detection system was used with commercially available probes (Table S3 for TaqMan and Table S4 for SYBR Green). *Ifn-α* and *Ifn-β* qPCR analysis was conducted on a CFX Connect Real Time PCR system (BioRad Laboratories, CA, USA) and all other gene analysis was conducted using a QuantStudio™ 6 real-time PCR system (Invitrogen). Results were analysed using QuantStudio™ software (Life Technologies, Version 1.1). Cycle threshold (Ct) values were normalised to the housekeeping gene Glyceraldehyde-3-phosphate dehydrogenase (Gapdh). Relative gene expression was calculated using the comparative C_T method (Schmittgen & Livak, 2008).

2.8 | Immunohistochemistry

Mice were anaesthetised via intraperitoneal administration of ketamine/xylazine (100 mg·kg^{-1}/xylazine (10 mg·kg^{-1}) and cardiac perfused with ice cold PBS followed by ice cold 4% paraformaldehyde.

Isolated brains were post-fixed in 5 mL of 4% paraformaldehyde overnight at 4°C and then placed in 30% sucrose solutionfor 48 h. The brains were then embedded in optimal cutting temperature media (OCT) (Sakura, Cat. No. 4583) and coronally sectioned at a thickness of 30 µm. Sections were washed three times with PBS on a rocker at 20RPM for 5 min each followed by 2-h incubation in blocking buffer containing 10% goat serum and 1% Tween-20. Following blocking, sections were rinsed in PBS followed by overnight incubation with primary antibody (Table S5) on a rocker at 20RPM at 4°C. Sections were then rinsed with PBS and incubated at room temperature for 1 h with secondary antibodies (Table S6). Sections were again rinsed three times with PBS followed by one rinse with milliQ H_20 before being mounted onto Superfrost plus™ slides (Thermo Scientific, Cat. No. SF41296SP) with Vectashield HardSet antifade mounting medium with DAPI. Slides were imaged using a Zeiss Observer Z1 widefield microscope and Zen 2.6 (Zeiss, blue edition) software (Data S1).

2.9 | Microglial morphological analysis

The quantification of microglial morphology performed in this study was based on a protocol previously described and reported by our group (Moore et al., 2020). Thirty-micrometre sagittal brain sections were collected and imaged using Zeiss Observer Z1 widefield microscope with 10× magnification. Three to five images were taken at the perilesional cortex and at the corresponding location on the contralateral cortex. Images underwent maximum intensity projections before analysis. Images were analysed using a proprietary spanning tree path finding based algorithm with a minimum of 50 microglia per image analysed (Abdolhoseini et al., 2016). Trace images were then analysed on Matlab v2013b using built-in functions. To ensure that only cells with visible major branches were included in the analysis, cells overlapped with each other or had contact with the image border were excluded from analysis.

2.10 | Data and statistical analysis

The data and statistical analysis comply with the recommendations of the *British Journal of Pharmacology* on experimental design and analysis in pharmacology (Curtis et al., 2022). All statistical analysis was conducted using GraphPad Prism version 8.4.2 for Windows. Data are presented as mean ± standard error of the mean (SEM). Statistical analysis was understaken for studies where each group size was at least n = 5 (where n refers to the number of independent data points). Sample size was determined by power analysis. A variance was set at 15% to determine a 25% significant difference that will require a group of eight or more animals for behavioural and infarct size analysis. For comparisons between two treatment groups, a two-tailed Student's *t*-test was used. For comparisons between three or more treatment groups, a one-way ANOVA with a Tukey's post hoc multiple comparisons test was used. Post-hoc tests were run only if F achieved $P < 0.05$ and there was no significant variance homogeneity. *P* values less than 0.05 were deemed statistically significant.

2.11 | Materials

The small-molecule STING inhibitor, n-(4-iodophenyl)-5-nitrofuran-2-carboxamide (C-176; Cat. No. EN300-6503757) was purchased from Enamine Ltd (Kyiv, UA). Powdered C-176 was dissolved in dimethyl sulfoxide (DMSO; Cat. No. BIOD0231) purchased from Astral Scientific (NSW, AUS) to achieve a final concentration of 10 mM. Aliquots of stock solution were stored at −20°C until required. Xylazine (Cat. No. X1251), goat serum (Cat. No. G9023), Tween-20 (Cat. No. P1379), Triton X-100 (Cat. No. T8787), sodium dodecyl sulphate (SDS; Cat. No. L3771), sodium deoxycholate (Cat. No. D6750), ethylenediaminetetraacetic acid (EDTA; Cat. No. E9884), 2-mercaptoethanol (Cat. No. M3148), cOmplete™ protease inhibitor cocktail tablet (Cat. No. 11697498001), PhosSTOP™ phosphatase inhibitor cocktail tablet (Cat. No. 4906845001) and polyvinylidene fluoride (PVDF) membranes (Cat. No. IPVH00010) were purchased from Merck Life Science (VIC, AUS). Buprenorphine was purchased from Lyppard Australia Pty Ltd (VIC, AUS). Tris-hydrochloride (Cat. No. BIOTB0103), sodium chloride (Cat. No. SA046) and paraformaldehyde (PFA; Cat. No. PA00950500) were purchased from Chem Supply (SA, AUS), while cyclic di-GMP (c-di-GMP) (Cat. No. tlrl-nacdg) was purchased from Invivogen (CA, USA). Dulbecco's modified eagle medium (DMEM; Cat. No. 11995-065), TRIzol™ reagent (Cat. No. 15-596-018) and phosphate-buffered saline (PBS; Cat. No. 18912014) were purchased from ThermoFisher Scientific (AUS). **DAPI** (Cat. No. H-1500) was purchased from Abacus dx (QLD, AUS), while wax coated braided silk (Cat. No. S-1173) was purchased from Medtronic (NSW, AUS). Details of other materials and suppliers were provided in the specific sections.

2.12 | Nomenclature of targets and ligands

Key protein targets and ligands in this article are hyperlinked to corresponding entries in the IUPHAR/BPS Guide to PHARMACOLOGY in http://www.guidetopharmacology.org/, and are permanently archived in the Concise Guide to PHARMACOLOGY 2022/2023 (Alexander, Kelly, Mathie et al., 2023; Alexander, Fabbro, Kelly et al. 2023).

3 | RESULTS

3.1 | C-176 attenuates STING activation in BV2 cells

To assess the efficacy of C-176 in inhibiting STING activation, we pre-treated BV2 microglia-like cells with 0.1–2 µM of C-176 followed by an 8-h incubation with 10–20 µg of STING agonist cyclic-di-GMP (Figure 1). Inhibition of c-di-GMP-induced STING and TBK1 phosphorylation was observed following incubation with 0.1-, 1- and 2-µM C-176, with complete inhibition of STING and TBK1 phosphorylation at a concentration of 2 µM of C-176 (Figure 1).

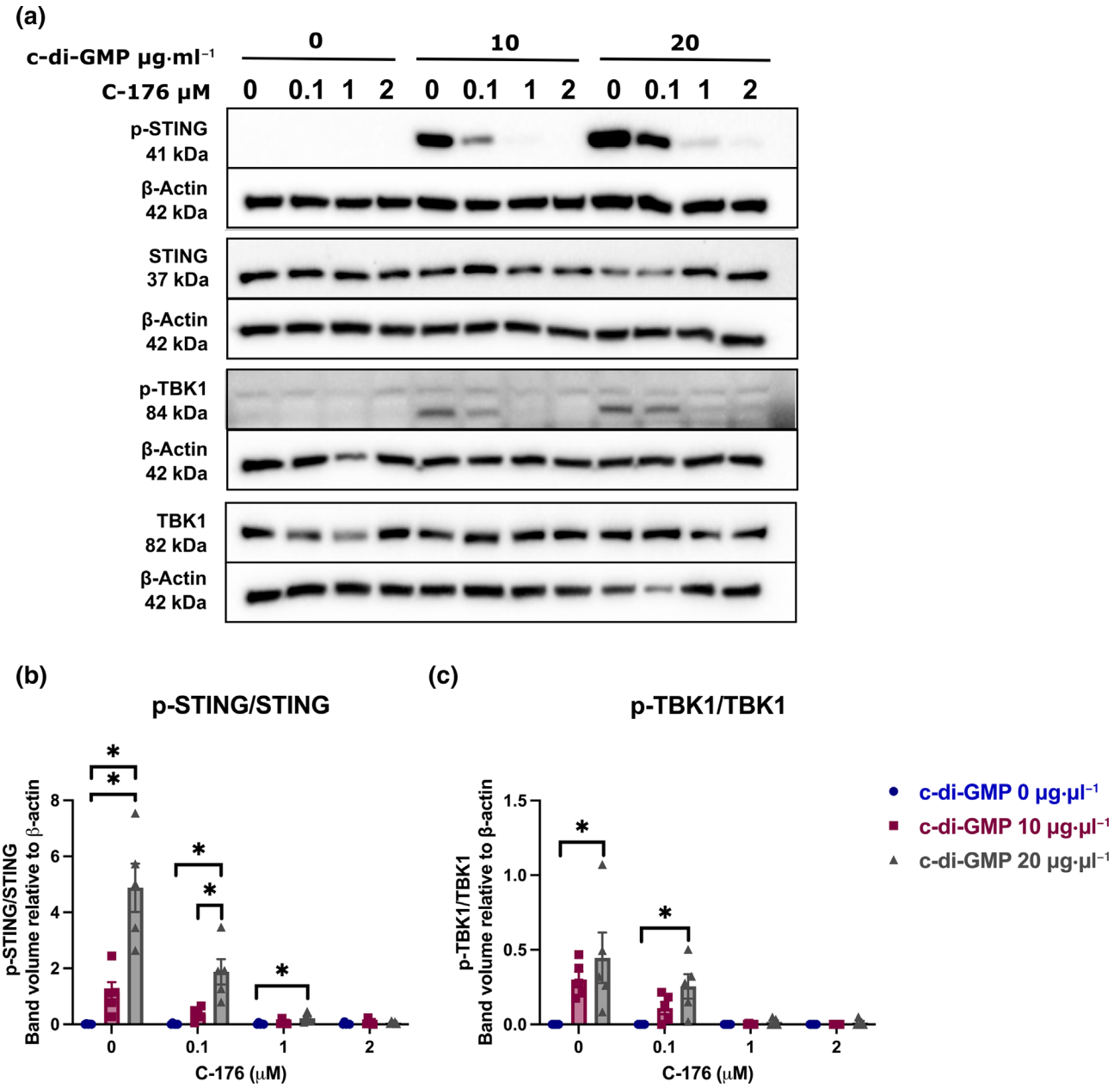

FIGURE 1 C-176 inhibits cyclic di-nucleotide (CDN)-mediated STING activation. Inhibition of STING and TBK1 phosphorylation occurs in BV2 microglia-like cells pre-treated for 30 min with 0.1–2 µM of STING inhibitor C-176 and treated for 8 h with 10–20 µg/mL of c-di-GMP. (a) Protein expression analysed by western blot. Densitometric analysis (b, c) was performed to quantitate expression of p-STING relative to STING and p-TBK1 relative to TBK1. Protein expression was measured as ratio of band intensity and β-actin loading control. The expression of p-STING (b) and p-TBK1 (c) was made relative to total protein expression of STING and TBK1, respectively. All data are expressed as mean ± SEM. STING phosphorylation was significantly increased following treatment with 10 $\mu g \cdot ml^{-1}$ ($P < 0.05$) and 20 $\mu g \cdot ml^{-1}$ ($P < 0.05$) of c-di-GMP compared to untreated vehicle. Treatment with 2-µM C-176 completely ablated c-di-GMP induced phosphorylation of STING. n = 5. Significance determined by one-way ANOVA followed by a Bonferroni's multiple comparison test within each dose of C-176. *$P < 0.05$.

3.2 | C-176 administration post-TBI reduces cortical lesion size

The effect of C-176 on trauma-induced neuroinflammation was assessed *in vivo* using the controlled cortical impact model of mild TBI. MRI imaging was conducted to evaluate cortical damage 24 h and 7 days post-TBI in mice intravenously injected 30 min post-TBI with a single 750-nmol dose of C-176 (C-176) or a saline-vehicle control (Vehicle). Quantification of the lesion area revealed that mice treated with C-176 had a 29% reduction in the area of damage in the cortex 24 h post-TBI compared to vehicle-treated TBI mice and a 24% reduction 7 days post-TBI (Figure 2).

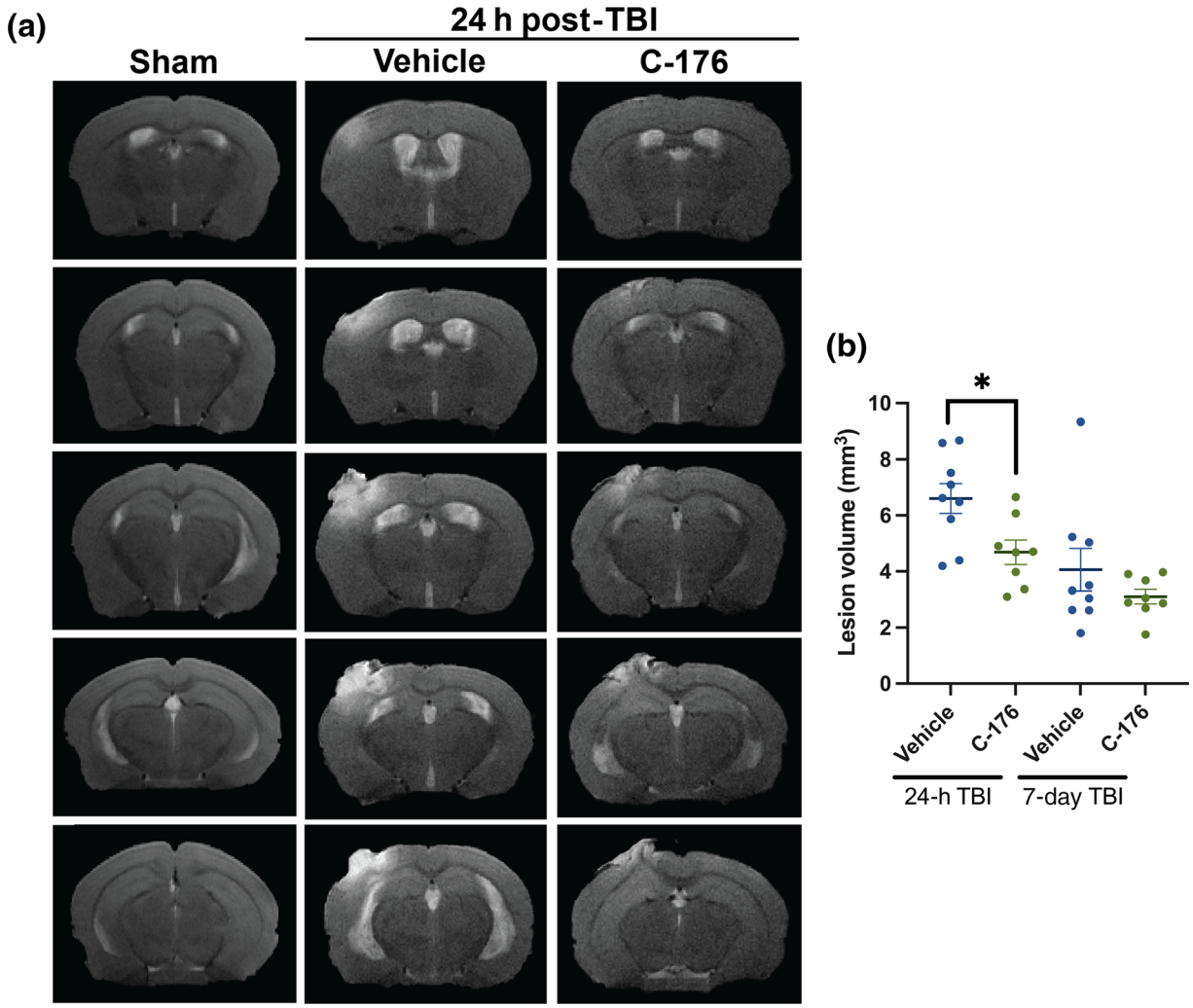

FIGURE 2 Administration of C-176 reduces traumatic brain injury (TBI)-induced brain lesion. MRI T2 images from C57BL/6 mice showing TBI lesion 24 h post-injury (a). Mild TBI was modelled using a controlled cortical impactor. Thirty minutes post-TBI, mice were intravenously administered a saline vehicle or STING inhibitor C-176. Sham mice underwent identical surgery omitting the TBI. Mice administered C-176 post-TBI had significantly reduced lesion volumes 24 h after injury (*$P < 0.05$) and no significant change in lesion volume 7 days post-injury (b). Data represents mean ± SEM, n = 8–9 animals per group. Significance was determined using unpaired two-tailed *t* test. *$P < 0.05$.

3.3 | Treatment with 750-nmol C-176 post-injury rescues gait disturbances in mice 24 h post-TBI

This study conducted a quantitative temporal gait analysis to gauge alterations in neurobehavioral activity following TBI in mice. Changes in gait parameters were measured using DigiGait™ (parameter definitions provided in Table 1). C-176 administration attenuated TBI-induced impairments in stride frequency (Figures 3e and 4e) and forelimb stance width (Figure 3d), in addition to restoring time spent in forelimb and hindlimb stance phase and stride phase to values similar to sham and statistically longer than vehicle-treated TBI mice (Figures 3b,c and 4b,c).

Furthermore, the vehicle-treated TBI mice displayed an elevated gait symmetry ratio compared to sham (Figure 3f). A gait symmetry value of 1 indicates co-ordinated movement in both the left and right side of the body. The gait symmetry measured in mice treated with C-176 after TBI was closer to 1 compared to vehicle-treated mice and was not statistically different to sham mice (Figure 3f). The sham and vehicle-treated TBI mice had similar hindlimb stance width, while mice treated with C-176 after TBI exhibited a narrower hindlimb stance width (Figure 4e).

3.4 | C-176 on STING expression after TBI

To evaluate the effect of single-dose C-176 administration on STING-mediated neuroinflammation, 2 h and 24 h post-TBI, protein and mRNA expression of STING and downstream mediators TBK1 and IRF3 were measured by western blot and qPCR analysis. Mice treated with C-176 did not display significant alterations in *Sting* mRNA expression in the cortex and striatum when compared to vehicle-treated mice at both 2 h and 24 h post-TBI (Figures S2F and

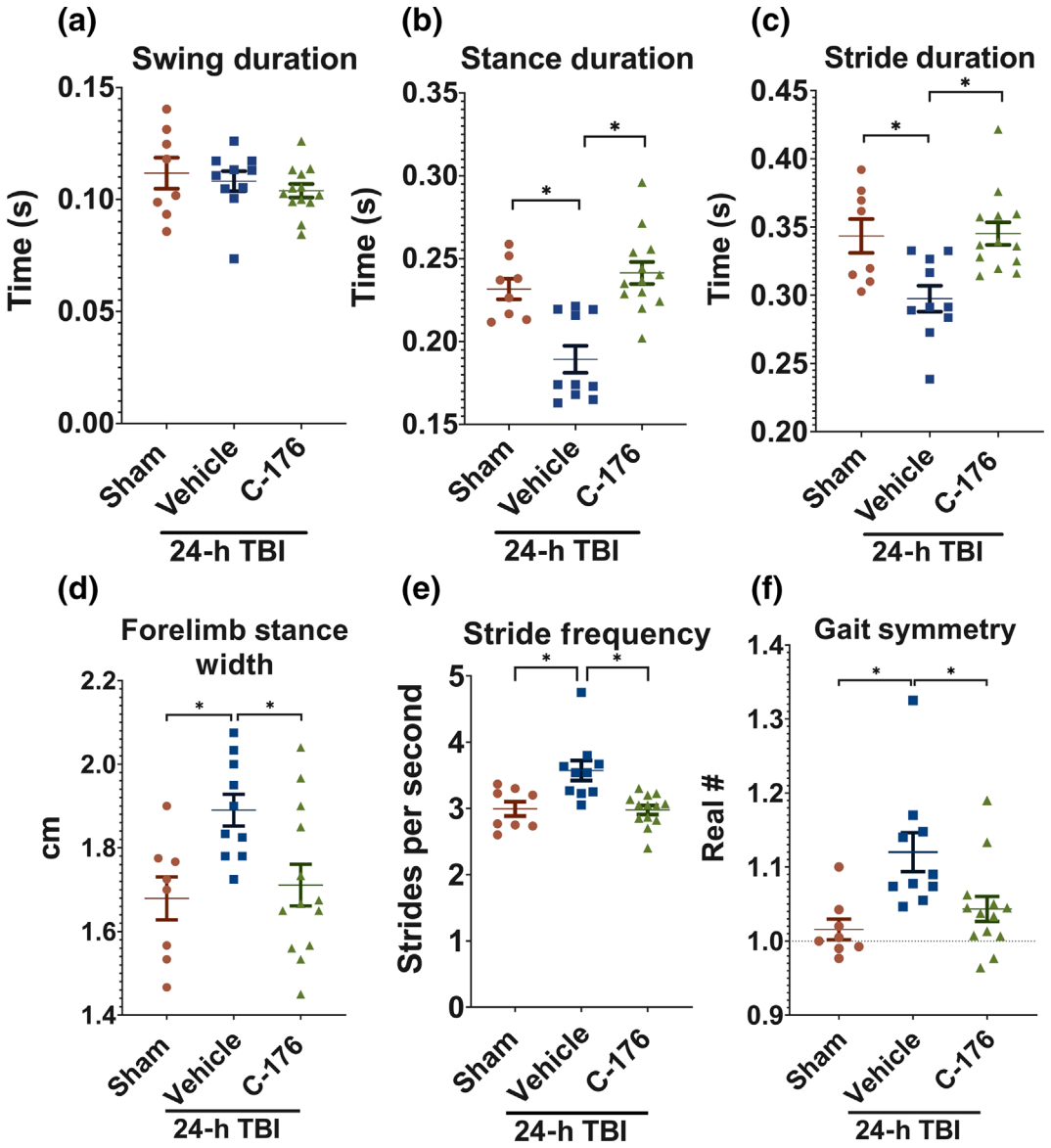

FIGURE 3 C-176 significantly improves left forelimb gait deficits 24 h post-traumatic brain injury (TBI). Quantitative temporal gait parameters of mice were measured using DigiGait™ imaging and analysis software 24 h after 1.5-mm impact controlled cortical impact surgery (TBI) and no impact (sham). No change in (a) swing duration was observed. Significant improvements found in (b) stance ($P < 0.05$) and (c) stride duration ($P < 0.05$), (d) forelimb stance width ($P < 0.5$) (e) stride frequency ($P < 0.05$) and (f) gait symmetry ($P < 0.05$) in TBI mice treated with 750-nmol STING inhibitor (C-176) compared to TBI mice treated with a vehicle. Sham n = 8, TBI-vehicle n = 10, TBI-C-176 n = 13. Data are presented as mean ± SEM. Significance determined by one-way ANOVA with Tukey's multiple comparison test. *$P < 0.05$.

S3F). *Irf3* mRNA expression in the striatum of C-176 treated mice significantly increased 2 h post-TBI when compared to vehicle-treated mice (Figure S2G) and remained relatively unchanged 24 h post-TBI (Figure S3G). Western blot analysis revealed that there were no significant changes in cortical STING protein expression observed 2 h post-TBI in C-176-treated mice compared to sham or vehicle-treated mice (Figure S2C). Interestingly, C-176-treated mice displayed significantly attenuated total TBK1 expression in the striatum 2 h post-TBI compared to sham (Figure S2C). Both C-176- and vehicle-treated mice had a reduction in the protein expression of STING and total and phosphorylated TBK1 in the cortex and striatum compared to sham 24 h post-TBI (Figure S3C–E).

3.5 | C-176 alters microglial density and does not influence microglial phenotype

Since we identified an alteration to *Sting* mRNA expression, TBK1 and p-TBK1 protein expression in vehicle-treated mice 24 h post-TBI, we wanted to elucidate if these changes also resulted in altered microglial activity. Immunohistochemical analysis was conducted on **CX_3CR1^{eGFP}** mice, which have fluorescently tagged microglia. Morphological analysis was conducted on CX_3CR1^{eGFP} mice 24 h post-TBI to quantify any phenotypical changes to the microglia that could indicate alterations to the inflammatory environment in the CNS. STING was found to strongly colocalise with CX_3CR1^{eGFP}-tagged microglia

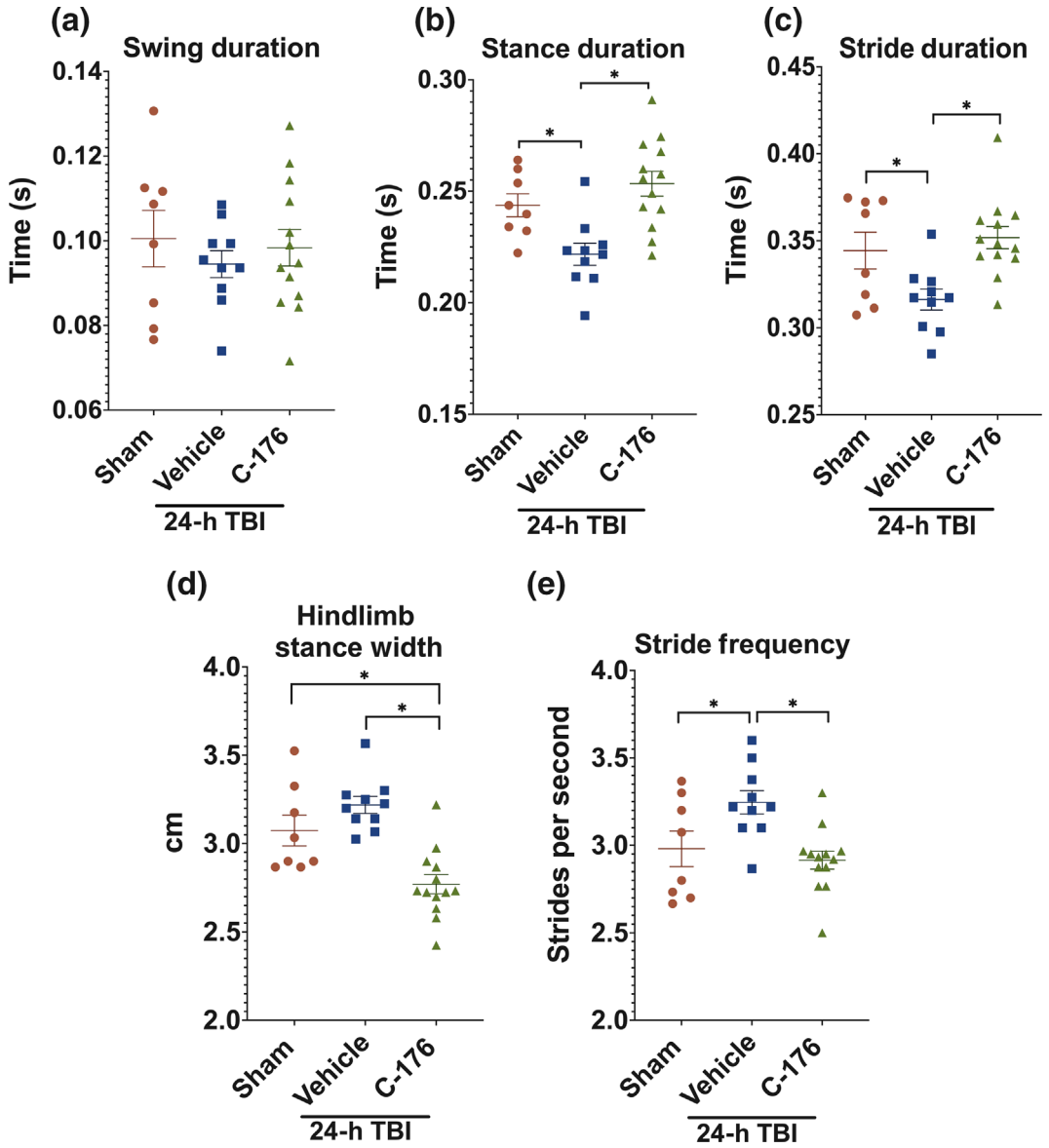

FIGURE 4 C-176 significantly improves left hindlimb gait deficits 24 h post-traumatic brain injury (TBI). Quantitative temporal gait parameters of mice were measured using DigiGait™ imaging and analysis software 24 h after 1.5-mm impact controlled cortical impact surgery (TBI) and no impact (sham). No change in swing duration between treatment groups was observed (a). Significant improvements found in (b) stance ($P < 0.05$) and (c) stride duration ($P < 0.05$) and (e) stride frequency ($P < 0.05$) in TBI mice treated with 750-nmol STING inhibitor (C-176) compared to TBI mice treated with a vehicle. (d) Hindlimb stance width in C-176-treated mice significantly lower than sham ($P < 0.05$) and vehicle-treated TBI mice ($P < 0.05$). Sham n = 8, TBI-vehicle n = 10, TBI-C-176 n = 13. Data are presented as mean ± SEM. Significance determined by one-way ANOVA with Tukey's multiple comparison test. *$P < 0.05$.

2 h post-TBI (Figure 5). The density of microglia was significantly lower in the contralateral cortex of C-176-treated mice compared to vehicle-treated mice 24 h post-TBI (Figure 6f). Microglia density was higher in the contralateral cortex compared to the ipsilateral cortex in vehicle-treated mice and unchanged in the C-176 mice (Figure 6f). There was a small increase in soma size detected post-TBI compared to the microglia contralateral to the TBI-lesion; however, no differences in total branch length, cell area or soma area were observed between vehicle-treated and C-176-treated mice post-TBI (Figure 6).

3.6 | Type-I IFN expression is elevated post-TBI and unaffected by C-176 administration

As STING in a regulator of type-I IFN activity, we wanted to evaluate if administration of C-176 alters *Ifn-α* and *β* gene expression in the CNS 2 h and 24 h post-injury. *Ifn-β* expression was significantly elevated in cortex and striatum of vehicle- and C-176-treated mice 2 h post-TBI when compared to sham mice (Figure 7a). *Ifn-α* was significantly elevated in C-176-treated mice

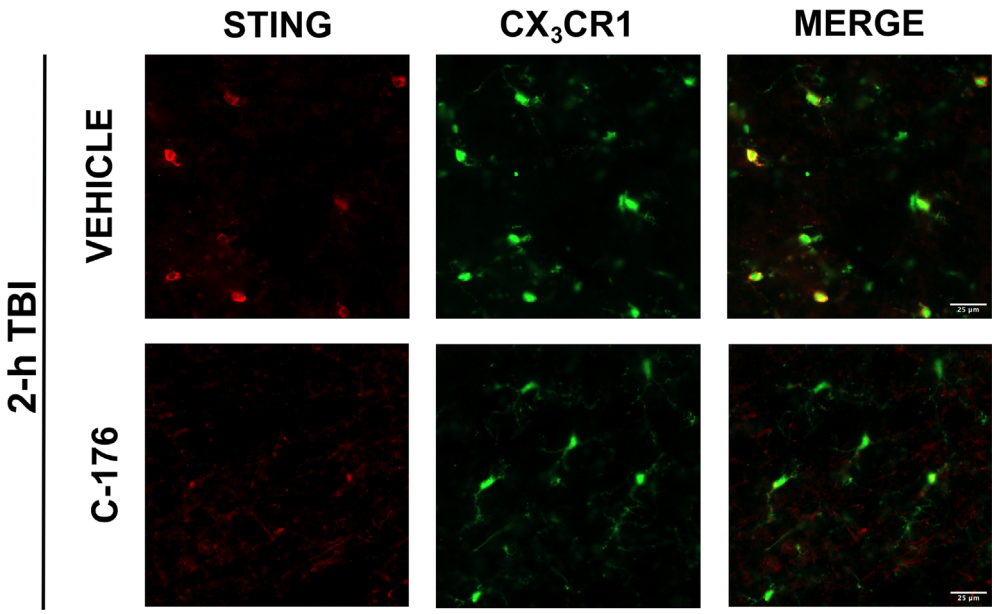

FIGURE 5 STING expression colocalises with microglia 2 h post-traumatic brain injury (TBI). Representative immunofluorescence images of STING (red) and GFP-tagged CX_3CR1 microglia (green) taken around lesion area 2 h post-TBI. Thirty minutes following TBI, mice were administered a saline vehicle (a) or a single 750-nmol dose of C-176 (b). Images taken on Zeiss Axio Observer 7.1 widefield microscope at 20× objective. Scale bar: 25 µm.

compared to sham 2 h and 24 h post-injury (Figure 7a,b). No change in both *Ifn-α* and *β* gene expression was detected between the vehicle-treated and C-176-treated mice 2 h and 24 h post-TBI (Figure 7).

3.7 | C-176 reduces TBI-induced pro-inflammatory cytokine response 2 h post-injury

To elucidate the effect of C-176 on the neuroinflammatory milieu post-TBI, gene expression of pro-inflammatory markers intimately related to the type-I IFN response was measured in the ipsilateral cortex and striatum regions of the brain at 2 h and 24 h post-TBI (Figure 8). Administration of C-176 significantly attenuated cortical expression of *CXCL10* 2 h post-TBI (Figure 8a, v) compared to vehicle-treated mice but did not have a marked effect on cortical expression of the other pro-inflammatory markers measured (Figure 8a, i–iv and vi). C-176-treated mice displayed a significant reduction in striatal gene expression of pro-inflammatory cytokines *Tnf-α*, *Il-1β* and *Cxcl10* compared to their vehicle-treated counterparts at 2 h post-TBI (Figure 8a, i, iii and v). Vehicle-treated mice 24 h post-TBI displayed significantly elevated expression of *Il-1β*, *Tnf-α* and *Cxcl10* in both the cortex and the striatum compared to sham (Figure 8b, i, iii and v). ***Il-6*** and ***Nos2*** expression increased in the vehicle-treated TBI mice in the cortex (Figure 8b, ii and iv). C-176-treated mice displayed significantly increased expression of *Tnf-α* in both the cortex and the striatum (Figure 8b, iii) and *Cxcl10* in the cortex compared to sham (Figure 8b, v). No significant difference in the expression of the pro-inflammatory markers measured was detected between the vehicle-treated mice and C-176-treated mice 24 h post-TBI (Figure 8b).

4 | DISCUSSION AND CONCLUSIONS

Traumatic brain injury (TBI) is often referred to as a 'silent epidemic', causing debilitating neurological deficits to millions of people globally each year (Dewan et al., 2019). Treatments limiting the damage caused by secondary injury processes following TBI are an area of severe unmet medical need (Carbonara et al., 2018; Khellaf et al., 2019). Medical intervention is limited to stabilisation of the patient via barbiturate coma and decompressive surgical intervention. The patient has little scope to improve neurological function and an extremely decreased quality of life (Cook et al., 2020; Galgano et al., 2017). After injury, the neural cells die from physical damage, eliciting a sequence of events that creates a neuroinflammatory microenvironment that prevents recovery. Neurodegeneration driven by complex, chronic and dysregulated neuroinflammation is particularly detrimental to the neurological recovery after TBI (Simon et al., 2017). cGAS-STING-IFN signalling is increasingly being appreciated as a driver of this neuroinflammation in rodent models of TBI (Abdullah et al., 2018; Fritsch et al., 2022; Wangler et al., 2022; Zhang et al., 2022). Here, we examine if pharmacological inhibition of STING can attenuate neuroinflammation and neurodegeneration post-TBI and lead to neuroprotection and improved behavioural outcome.

We firstly identified that C-176 can successfully inhibit STING activation in glial cells *in vitro* in BV2 microglia-like cells (Figure 1). Importantly, this identified that C-176 was targeting STING activation. We then employed a single-dose administration of this STING inhibitor in our mouse model of mild-TBI. It was evident that single-dose administration of C-176 post-TBI in our mouse model was able to confer neuroprotection. The timepoint of 30 min was chosen in this study to represent the 'golden hour' in which intervention for TBI may have the most beneficial effects. It is important to note that

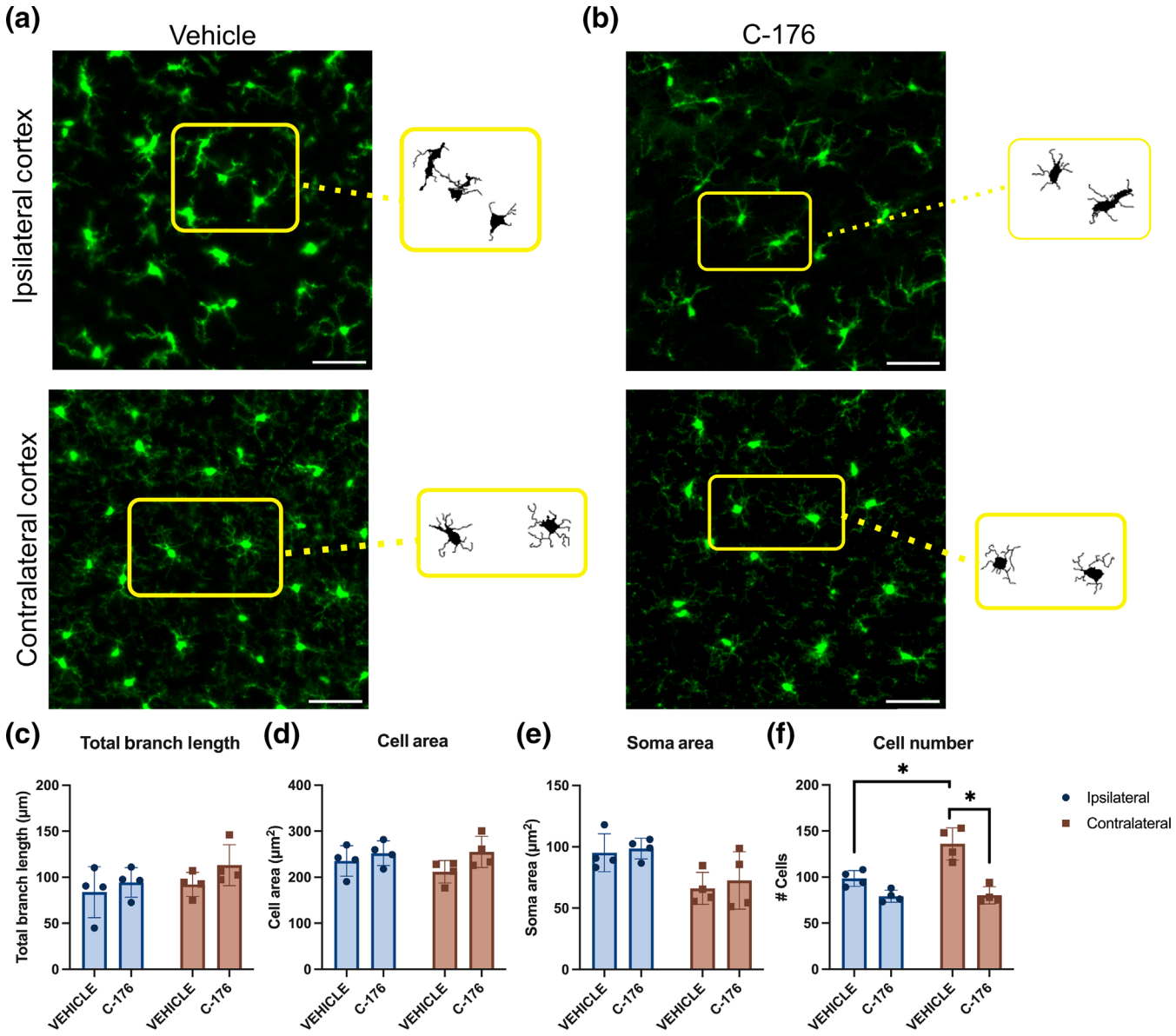

FIGURE 6 Administration of C-176 alters microglial density and does not alter microglial morphology 24 h-post traumatic brain injury (TBI). 30µm-thick brain sections of CX_3CR1^{eGFP} mice subjected to controlled cortical impact TBI. Representative images are shown for the ipsilateral and contralateral cortex of vehicle-treated (a) and C-176-treated (b) mice with an overview of the skeletonising process employed using a minimum spanning tree algorithm to measure morphological characteristics. Administration of C-176 did not significantly alter (c) total branch length, (d) cell area and (e) soma area of perilesional microglia compared to vehicle treated mice 24 h post-TBI. Administration of C-176 significantly decreased the number of CX_3CR1-tagged microglia in the contralateral cortex (f). Each data point is an average of 200–500 cells. Scale bar = 50 µm. n = 5 for each group. Significance determined by one-way ANOVA with Tukey's multiple comparison test. *$P < 0.05$.

in developed countries such as England and Wales, the median time to intervention for patients post-severe and moderate TBI is 0.5–0.9 h (Lawrence et al., 2016). Mice treated with C-176 displayed significantly smaller lesion areas 24 h post-TBI (Figure 2). These results are comparable with previous findings by our group using *Sting*$^{-/-}$ mice, which highlighted that deletion of STING resulted in neuroprotection after TBI (Abdullah et al., 2018). These results are also consistent with the work conducted by Zhang et al. (2022), where administration of C-176 in a rat model of severe TBI showed attenuated neuronal loss around the lesion site 24 h post-TBI. Additionally, use of C-176 in a mouse model of stroke was also found to significantly reduce infarct size 24 h after stroke modelling (Kong et al., 2022). Our neurobehavioral findings further confirm the neuroprotective capability of C-176 post-TBI. We found that TBI-induced gait deficits were reversed following C-176 administration (Figures 3 and 4). Studies using C-176 in rodent models of severe TBI and ischemic stroke have all found similar improvements in neurological and cognitive function suggesting that this compound could be beneficial in alleviating acute neurological symptoms (Kong et al., 2022; Zhang et al., 2022).

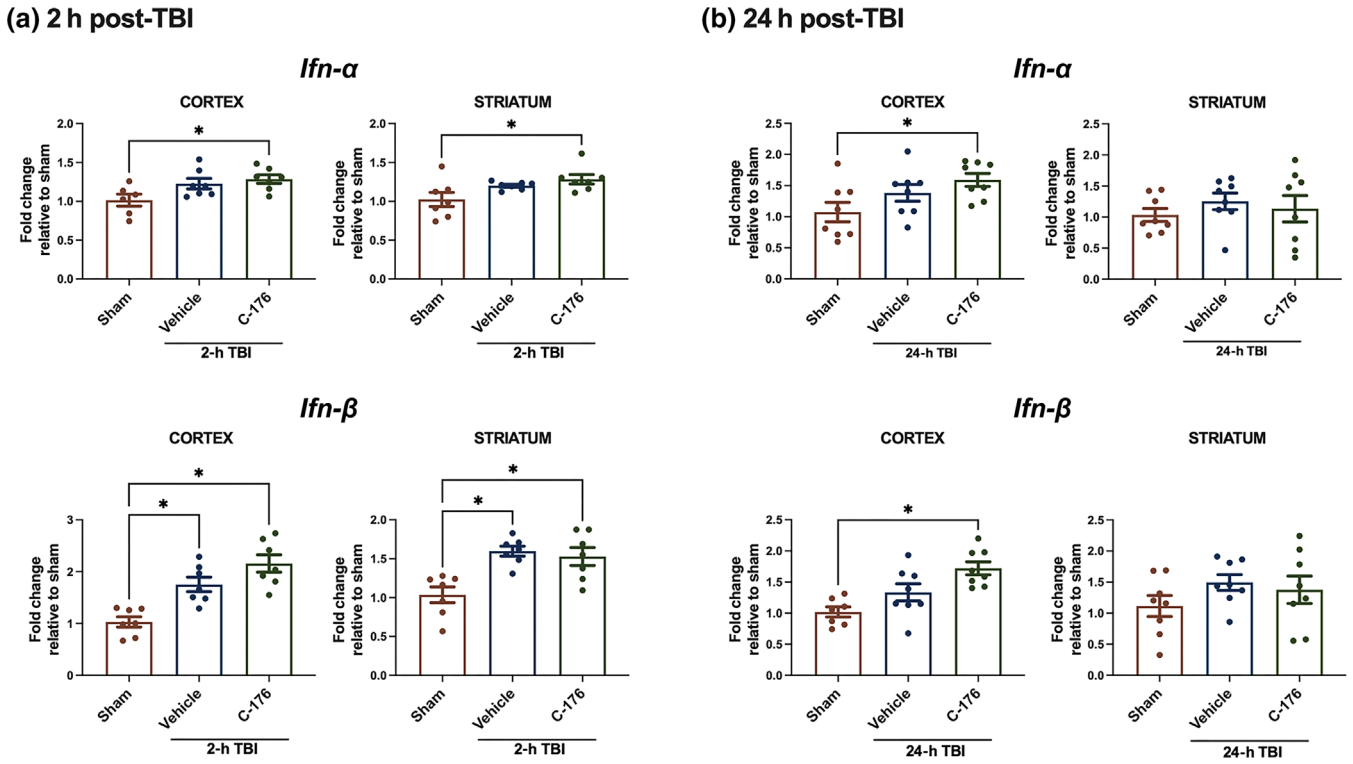

FIGURE 7 Type-I IFN expression is elevated post-traumatic brain injury (TBI) and unaffected by C-176 administration. Gene expression as measured by qPCR of *Ifn-α* and *Ifn-β* in the ipsilateral cortex and striatum isolated 2 h (a) and 24 h post-controlled cortical impact modelled TBI (b) and intravenous administration with C-176 or a saline vehicle. Sham mice underwent identical surgery omitting the cortical impact. No significant change in *Ifn-α* and *Ifn-β* expression was detected between vehicle-treated and C-176-treated mice 2 h and 24 h post-TBI. *Ifn-α* and *Ifn-β* expression was significantly elevated in C-176-treated mice in the cortex (*Ifn-α* $P < 0.05$, *Ifn-β* $P < 0.05$) and striatum 2 h post-TBI compared to sham. Cortical expression of *Ifn-α* and *Ifn-β* was elevated in C-176-treated mice (*Ifn-α* $P < 0.05$, *Ifn-β* $P < 0.05$) and not vehicle-treated mice 24 h post-TBI compared to sham. All data are presented as mean ± SEM. n = 6–7 (2 h post-TBI), n = 9 (24 h-TBI). Significance was determined for the cortex and striatum separately using a one-way ANOVA and Tukey's multiple comparison test. *$P \leq 0.05$.

Previous studies have identified microglia as a key source of STING activity in the CNS (Ding et al., 2022; Mathur et al., 2017; Wangler et al., 2022). Following TBI, microglia are known to migrate to the site of injury and undergo rapid proliferation with morphological and functional changes (Davalos et al., 2005; Witcher et al., 2021). We were able to confirm that STING expression was predominately located in microglial cells post-TBI (Figure 5). We are the first to assess microglial morphology following administration of C-176 and found that administration of C-176 did not elicit any morphological changes in the perilesional microglia between C-176-treated mice and their vehicle counterparts (Figure 6). We did find that mice treated with C-176 displayed a lower cortical density of microglia, suggesting that C-176 may enact its neuroprotective activity by attenuating microglial proliferation and migration post-TBI (Figure 6). Work conducted by Zhang et al. (2022) found that administration of C-176 reduced the co-localisation of STING in microglia and astrocytes 32 days post-severe TBI. This suggests that there may be more significant morphological changes occurring in microglia at a timepoint later than the one used in the present study (24 h post-TBI). This result also highlights that early administration of a STING inhibitor may be important in limiting the acute morphological and biochemical changes that occur in microglia after TBI.

Mild TBI and single-dose administration of C-176 was found to alter the neuroinflammatory profile in the cortex and striatum 2 and 24 h post-TBI. The anti-inflammatory effects of the C-176 post-TBI were observed acutely post-injury and had most observable attenuation of expression of pro-inflammatory genes *Il-1β*, *Cxcl10* and *Tnf-α* in the striatum 2 h post-injury (Figure 8a, ii, iii and v). Previous work by our group has demonstrated that haematopoietic cells play a key role in the neuroinflammatory response in this model (Karve et al., 2016). Neuroinflammation is a hallmark of various neurological disorders, including TBI (DiSabato et al., 2016). Activation of the STING pathway in microglia and astrocytes contributes significantly to the production of pro-inflammatory mediators, such as *TNF-α*, *IL-1β* and *IL-6*, which exacerbate neuroinflammation (Abdullah et al., 2018; Nazmi et al., 2019). The STING pathway has been shown to amplify the inflammatory response by inducing the nuclear factor-kappa B (NF-κB) pathway, a master regulator of inflammation and inflammasome activation (Tanaka & Chen, 2012). Future work would investigate if C-176 is acting through these peripheral cells to elicit the neuroprotective anti-inflammatory effect we have observed.

Gene expression post-TBI of the key type-I IFNs, *Ifn-α* and *Ifn-β* was not affected by C-176 treatment (Figure 7). This finding highlights the complexity of targeting the STING-IFN axis as we found that

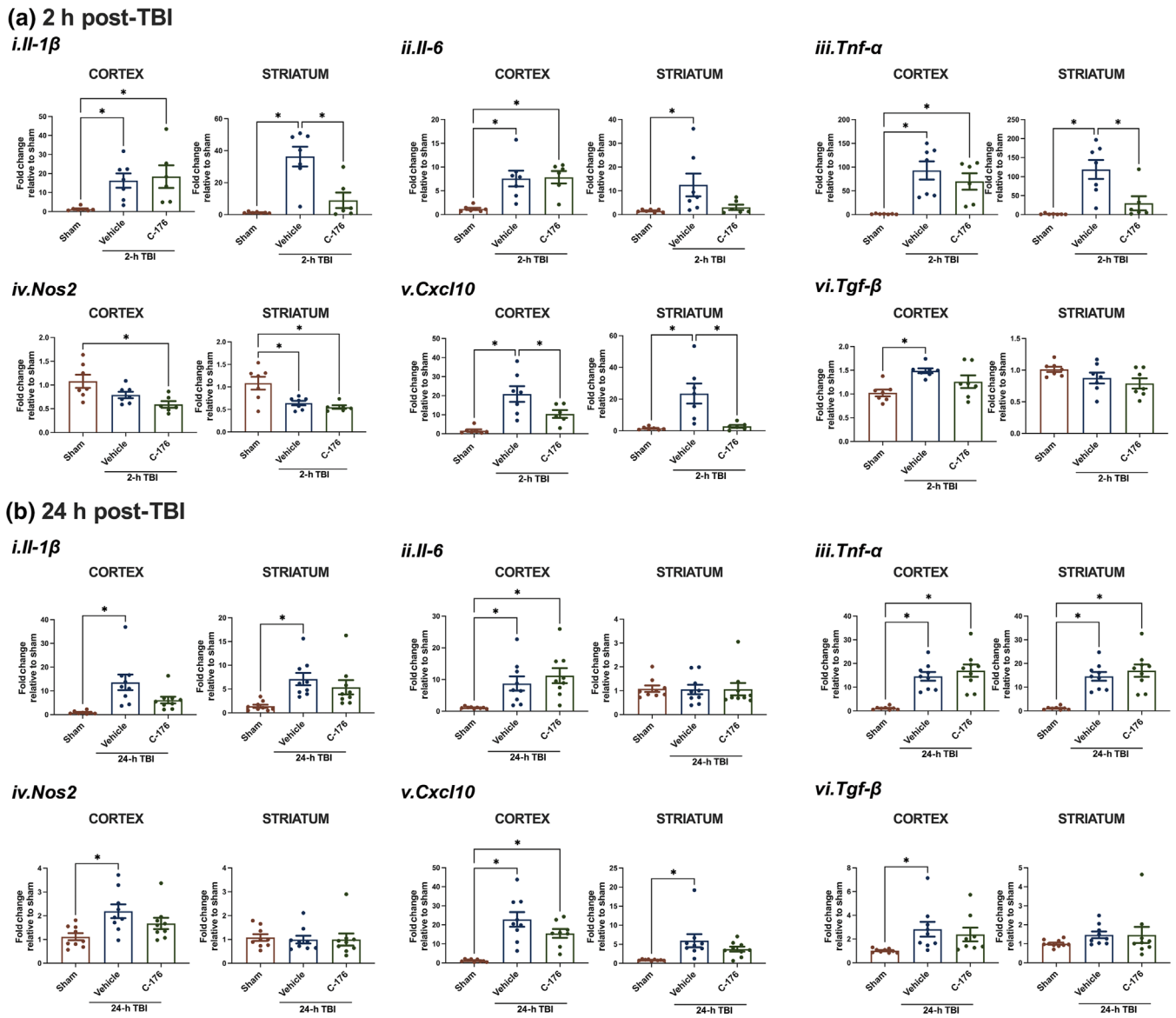

FIGURE 8 Gene expression of pro-inflammatory markers 2 h and 24 h following traumatic brain injury (TBI) and C-176 administration in mice. Gene expression as measured by qPCR of pro-inflammatory markers in the ipsilateral cortex and striatum isolated 2 h (a) and 24 h post-controlled cortical impact modelled TBI (b) and intravenous administration with C-176 or a saline vehicle. Two hours post-TBI (a), a significant increase in the cortical expression of *Il-1β* (i), *Tnf-α* (iii), *Cxcl10* (v) and *Tgf-β* (vi) was observed b. No significant change in the expression of *Il-6* (ii) was found. C-176-treated mice had significant attenuation of *Nos2* expression compared to sham in the cortex and striatum (iv) and significantly reduced expression of Cxcl10 (v) compared to vehicle treated mice in the cortex ($P < 0.05$) and striatum ($P < 0.05$). Twenty-four hours post-TBI (b), vehicle-treated mice increased cortical expression of *Il-1β* (i), *Il-6* (ii), *Nos2* (iv) and *Tgf-β* (iii). C-176-treated mice displayed an increase in the expression of *Tnf-α* (iii) in the cortex and striatum and *Cxcl10* in the cortex (v). All data are presented as mean ± SEM. n = 6–7 (2 h post-TBI), n = 9 (24 h post-TBI). Significance was determined for the cortex and striatum separately using a one-way ANOVA and Tukey's multiple comparison test. *$P \leq 0.05$.

C-176 markedly attenuates the expression of neuroinflammatory markers such as Il-1β that are known to be regulated by type-I IFNs (Figure 8). Emerging evidence is increasingly unveiling IFN-independent activities of STING in cellular processes like autophagy, cell death and proliferation (Wu et al., 2020). Our findings suggest that C-176 maybe eliciting its neuroprotective effect independently of type-I IFN signalling. A common concern surrounding the inhibition of immune regulators such as STING is the increased susceptibility to infection and cancer due to a dampened immune system. Our findings suggest that while STING is inhibited and neuroinflammation is attenuated following C-176 treatment, the type-I IFN response can remain intact. This supports STING as a promising therapeutic target to control the neuroinflammatory response post-TBI.

We did not observe changes to the total protein expression of STING 2 h post-TBI or C-176 administration (Figure S2). Interestingly, we found significantly attenuated STING, TBK1 and p-TBK1 24 h

post-TBI. We did not however find any significant changes between the vehicle-treated TBI mice and the C-176-treated mice. Work conducted by Zhang et al. (2022) using C-176 in a rat model of severe TBI found increased p-TBK1 and TBK1 expression in isolated hippocampus 24 h post-TBI, and C-176 was found to significantly decrease this p-TBK1 expression. We did observe an increase in the mRNA expression of STING in the cortex and striatum of the vehicle-treated TBI mice 24 h post-TBI and not at 2 h post-TBI. Together, this highlights the temporal sensitivity of STING activation in the CNS. Future studies should evaluate STING activation at later timepoints in addition to evaluating the expression in isolated hippocampus to further understand the effect of C-176 on STING activation in the CNS post-TBI.

Future studies will explore the pharmacokinetics of C-176 to address if its neuroprotective anti-inflammatory is occurring solely in the CNS or if it is acting on STING in peripheral immune cells. Furthermore, C-176 has been recorded to possess a short half-life when used in mice, thereby reinforcing the need to explore dosage frequency, concentration and timing to achieve optimal therapeutic effect (Haag et al., 2018). Future studies can provide more insight into the therapeutic window of using STING inhibitors by broadening the dosage concentration, frequency, timing and route of administration tested in this mouse model.

A limitation of this study is that we have not assessed the potential toxicity of C-176. C-176 may not act exclusively in the CNS and thus, it is important to consider possible off-target effects and long-term implications of attenuating inflammation *in vivo*. C-176 was discovered and characterised *in vivo* by Haag et al. (2018). As characteristic of small-molecule compounds, C-176 possesses a short serum half-life (Haag et al., 2018), which makes it advantageous for the modulation of STING as its inhibitory activity is transient and potentially allows for fine control of the immunosuppressive activity of C-176. Initial rodent toxicity studies by Haag and colleagues have confirmed C-176 to be well tolerated. Daily dosage of C-176 on wildtype mice over a 2-week period found no alterations to body weight or plasma levels of inflammatory markers TNF-α and IL-6. Additionally, the authors found no change to the red and white blood cell count, plasma or haemoglobin concentration. The authors found that daily administration of C-176 over a 2-week period does not induce liver or kidney toxicity (Haag et al., 2018). Furthermore, other studies using C-176 in mice have reported no observable adverse effects (Peng et al., 2020; Sun et al., 2022; Yu et al., 2023). As STING agonists are currently in clinical trials to combat cancer (Huang et al., 2022), we acknowledge that future toxicity testing beyond 2 weeks would provide valuable information as to the potential carcinogenic or pathogenic side effects that would arise from inhibiting STING *in vivo*.

This study has demonstrated a neuroprotective role of small-molecule inhibition of STING following mild TBI in mice, supporting additional studies investigating the therapeutic intervention of this pathway to address the severe unmet medical need of limiting the cell damage and functional deficits in TBI patients. The social and economic burden of brain injury is considerable to the community. New pharmacological tools are urgently needed to help delineate the neuroinflammatory pathways post-TBI and determine the most advantageous therapeutic window for the acute treatment of TBI.

AUTHOR CONTRIBUTIONS

A. L. Fryer: Data curation (lead); formal analysis (lead); investigation (lead); methodology (lead); writing—original draft (lead); writing—review and editing (lead). **A. Abdullah:** Data curation (equal); formal analysis (equal); investigation (equal); methodology (equal). **F. Mobilio:** Formal analysis (supporting); investigation (supporting); writing—review and editing (supporting). **A. I. Jobling:** Formal analysis (supporting); investigation (supporting). **Z. Moore:** Formal analysis (supporting); investigation (supporting). **M. de Veer:** Data curation (supporting); formal analysis (supporting); methodology (supporting); writing—review and editing (supporting). **G. Zheng:** Formal analysis (supporting); methodology (supporting). **B. X. Wong:** Formal analysis (supporting); investigation (supporting); supervision (supporting). **J. M. Taylor:** Conceptualization (equal); investigation (equal); project administration (equal); supervision (equal); writing—review and editing (equal). **P. J. Crack:** Conceptualization (lead); data curation (equal); formal analysis (supporting); funding acquisition (lead); investigation (supporting); project administration (lead); resources (lead); supervision (lead); writing—original draft (equal); writing—review and editing (equal).

ACKNOWLEDGEMENTS

This work was supported by grants from the National Health and Medical Research Council of Australia (NHMRC; Project Grant 1156744) to P.J.C and the Brain Foundation to A.A. We would like to thank the staff of the Melbourne Bioresources Platform for their expertise. Open access publishing facilitated by The University of Melbourne, as part of the Wiley - The University of Melbourne agreement via the Council of Australian University Librarians.

CONFLICT OF INTEREST STATEMENT

The authors report no competing interests.

DATA AVAILABILITY STATEMENT

The data that support the findings of this study are available from the corresponding author upon request.

DECLARATION OF TRANSPARENCY AND SCIENTIFIC RIGOUR

This declaration acknowledges that this paper adheres to the principles for transparent reporting and scientific rigour of preclinical research as stated in the *BJP* guidelines for Design and Analysis, Immunoblotting and Immunochemistry and Animal Experimentation, and as recommended by funding agencies, publishers and other organisations engaged with supporting research.

ORCID

Amelia L. Fryer https://orcid.org/0009-0005-6585-8520
Amar Abdullah https://orcid.org/0000-0001-9393-6032
Frank Mobilio https://orcid.org/0000-0002-5803-8488
Andrew Jobling https://orcid.org/0000-0002-7827-3135

Zachery Moore https://orcid.org/0000-0002-0898-0483
Michael de Veer https://orcid.org/0000-0001-8017-4155
Gang Zheng https://orcid.org/0009-0005-7320-5685
Bruce X. Wong https://orcid.org/0000-0002-1687-4138
Juliet M. Taylor https://orcid.org/0000-0002-4596-6760
Peter J. Crack https://orcid.org/0000-0002-5030-0330

REFERENCES

Abdolhoseini, M., Walker, F., & Johnson, S. (2016). Automated tracing of microglia using multilevel thresholding and minimum spanning trees. In *Proceedings of the annual international conference of the IEEE engineering in medicine and biology society* (pp. 1208–1211). EMBS.

Abdullah, A., Zhang, M., Frugier, T., Bedoui, S., Taylor, J. M., & Crack, P. J. (2018). STING-mediated type-I interferons contribute to the neuroinflammatory process and detrimental effects following traumatic brain injury. *Journal of Neuroinflammation*, *15*, 17.

Ablasser, A., Goldeck, M., Cavlar, T., Deimling, T., Witte, G., Röhl, I., Hopfner, K. P., Ludwig, J., & Hornung, V. (2013). cGAS produces a 2′-5′-linked cyclic dinucleotide second messenger that activates STING. *Nature*, *498*, 380–384. https://doi.org/10.1038/nature12306

Alexander, S. P. H., Kelly, E., Mathie, A. A., Peters, J. A., Veale, E. L., Armstrong, J. F., Buneman, O. P., Faccenda, E., Harding, S. D., Spedding, M., Cidlowski, J. A., Fabbro, D., Davenport, A. P., Striessnig, J., Davies, J. A., Ahlers-Dannen, K. E., Alqinyah, M., Arumugam, T. V., Bodle, C., … Zolghadri, Y. (2023). The Concise Guide to PHARMACOLOGY 2023/24: Introduction and Other Protein Targets. *British Journal of Pharmacology*, *180*, S1–S22. https://doi.org/10.1111/bph.16176

Alexander, S. P. H., Fabbro, D., Kelly, E., Mathie, A. A., Peters, J. A., Veale, E. L., Armstrong, J. F., Faccenda, E., Harding, S. D., Davies, J. A., Beuve, A., Brouckaert, P., Bryant, C., Burnett, J. C., Farndale, R. W., Friebe, A., Garthwaite, J., Hobbs, A. J., Jarvis, G. E., … Waldman, S. A. (2023). The Concise Guide to PHARMACOLOGY 2023/24: Catalytic receptors. *British Journal of Pharmacology*, *180*, S241–S288. https://doi.org/10.1111/bph.16180

Alexander, S. P. H., Roberts, R. E., Broughton, B. R. S., Sobey, C. G., George, C. H., Stanford, S. C., Cirino, G., Docherty, J. R., Giembycz, M. A., Hoyer, D., Insel, P. A., Izzo, A. A., Ji, Y., MacEwan, D., Mangum, J., Wonnacott, S., & Ahluwalia, A. (2018). Goals and practicalities of immunoblotting and immunohistochemistry: A guide for submission to the *British Journal of Pharmacology*. *British Journal of Pharmacology*, *175*, 407–411. https://doi.org/10.1111/bph.14112

Alosco, M. L., Tripodis, Y., Baucom, Z. H., Mez, J., Stein, T. D., Martin, B., Haller, O., Conneely, S., McClean, M., Nosheny, R., Mackin, S., McKee, A., Weiner, M. W., & Stern, R. A. (2020). Late contributions of repetitive head impacts and TBI to depression symptoms and cognition. *Neurology*, *95*, e793–e804. https://doi.org/10.1212/WNL.0000000000010040

Barrett, J. P., Henry, R. J., Shirey, K. A., Doran, S. J., Makarevich, O. D., Ritzel, R. M., Vogel, S. N., Faden, A. I., Stoica, B. A., & Loane, D. J. (2020). Interferon-beta plays a detrimental role in experimental traumatic brain injury by enhancing Neuroinflammation that drives chronic neurodegeneration. *The Journal of Neuroscience*, *40*, 2357–2370. https://doi.org/10.1523/JNEUROSCI.2516-19.2020

Carbonara, M., Fossi, F., Zoerle, T., Ortolano, F., Moro, F., Pischiutta, F., Zanier, E. R., & Stocchetti, N. (2018). Neuroprotection in traumatic brain injury: Mesenchymal stromal cells can potentially overcome some limitations of previous clinical trials. *Frontiers in Neurology*, *9*, 885. https://doi.org/10.3389/fneur.2018.00885

Chen, Q., Sun, L., & Chen, Z. J. (2016). Regulation and function of the cGAS-STING pathway of cytosolic DNA sensing. *Nature Immunology*, *17*, 1142–1149. https://doi.org/10.1038/ni.3558

Cook, A. M., Morgan Jones, G., Hawryluk, G. W. J., Mailloux, P., McLaughlin, D., Papangelou, A., Samuel, S., Tokumaru, S., Venkatasubramanian, C., Zacko, C., Zimmermann, L. L., Hirsch, K., & Shutter, L. (2020). Guidelines for the acute treatment of cerebral edema in Neurocritical care patients. *Neurocritical Care*, *32*, 647–666. https://doi.org/10.1007/s12028-020-00959-7

Corps, K. N., Roth, T. L., & McGavern, D. B. (2015). Inflammation and neuroprotection in traumatic brain injury. *JAMA Neurology*, *72*, 355–362. https://doi.org/10.1001/jamaneurol.2014.3558

Crow, Y. J., Hayward, B. E., Parmar, R., Robins, P., Leitch, A., Ali, M., Van Bokhoven, H., Brunner, H. G., Hamel, B. C., Corry, P. C., Cowan, F. M., Frints, S. G., Klepper, J., Livingston, J. H., Lynch, S. A., Massey, R. F., Meritet, J. F., Michaud, J. L., Ponsot, G., … Lindahl, T. (2006). Mutations in the gene encoding the 3′-5′ DNA exonuclease TREX1 cause Aicardi-Goutieres syndrome at the AGS1 locus. *Nature Genetics*, *38*, 917–920. https://doi.org/10.1038/ng1845

Curtis, M. J., Alexander, S. P. H., Cirino, G., George, C. H., Kendall, D. A., Insel, P. A., Izzo, A. A., Ji, Y., Panettieri, R. A., Patel, H. H., Sobey, C. G., Stanford, S. C., Stanley, P., Stefanska, B., Stephens, G. J., Teixeira, M. M., Vergnolle, N., & Ahluwalia, A. (2022). Planning experiments: Updated guidance on experimental design and analysis and their reporting III. *British Journal of Pharmacology*, *179*, 3907–3913. https://doi.org/10.1111/bph.15868

Davalos, D., Grutzendler, J., Yang, G., Kim, J. V., Zuo, Y., Jung, S., Littman, D. R., Dustin, M. L., & Gan, W. B. (2005). ATP mediates rapid microglial response to local brain injury in vivo. *Nature Neuroscience*, *8*, 752–758. https://doi.org/10.1038/nn1472

Dewan, M. C., Rattani, A., Gupta, S., Baticulon, R. E., Hung, Y. C., Punchak, M., Agrawal, A., Adeleye, A. O., Shrime, M. G., Rubiano, A. M., Rosenfeld, J. V., & Park, K. B. (2019). Estimating the global incidence of traumatic brain injury. *Journal of Neurosurgery*, *130*, 1080–1097. https://doi.org/10.3171/2017.10.JNS17352

Ding, R., Li, H., Liu, Y., Ou, W., Zhang, X., Chai, H., Huang, X., Yang, W., & Wang, Q. (2022). Activating cGAS-STING axis contributes to neuroinflammation in CVST mouse model and induces inflammasome activation and microglia pyroptosis. *Journal of Neuroinflammation*, *19*, 137. https://doi.org/10.1186/s12974-022-02511-0

DiSabato, D. J., Quan, N., & Godbout, J. P. (2016). Neuroinflammation: The devil is in the details. *Journal of Neurochemistry*, *139*, 136–153. https://doi.org/10.1111/jnc.13607

Dixon, K. J. (2017). Pathophysiology of traumatic brain injury. *Physical Medicine and Rehabilitation Clinics of North America*, *28*, 215–225. https://doi.org/10.1016/j.pmr.2016.12.001

Ek, C. J., Habgood, M. D., Callaway, J. K., Dennis, R., Dziegielewska, K. M., Johansson, P. A., Potter, A., Wheaton, B., & Saunders, N. R. (2010). Spatio-temporal progression of grey and white matter damage following contusion injury in rat spinal cord. *PLoS ONE*, *5*(8), e12021. https://doi.org/10.1371/journal.pone.0012021

Feng, X., Liu, D., Li, Z., & Bian, J. (2020). Bioactive modulators targeting STING adaptor in cGAS-STING pathway. *Drug Discovery Today*, *25*, 230–237. https://doi.org/10.1016/j.drudis.2019.11.007

Fritsch, L. E., Ju, J., Gudenschwager Basso, E. K., Soliman, E., Paul, S., Chen, J., Kaloss, A. M., Kowalski, E. A., Tuhy, T. C., Somaiya, R. D., Wang, X., Allen, I. C., Theus, M. H., & Pickrell, A. M. (2022). Type I interferon response is mediated by NLRX1-cGAS-STING signaling in brain injury. *Frontiers in Molecular Neuroscience*, *15*, 852243. https://doi.org/10.3389/fnmol.2022.852243

Fu, J., Kanne, D. B., Leong, M., Glickman, L. H., McWhirter, S. M., Lemmens, E., Mechette, K., Leong, J. J., Lauer, P., Liu, W., & Sivick, K. E. (2015). STING agonist formulated cancer vaccines can cure established tumors resistant to PD-1 blockade. *Science Translational Medicine*, *7*, 283ra52.

Galgano, M., Toshkezi, G., Qiu, X., Russell, T., Chin, L., & Zhao, L.-R. (2017). Traumatic brain injury: Current treatment strategies and future

endeavors. *Cell Transplantation*, *26*, 1118–1130. https://doi.org/10.1177/0963689717714102

Gonugunta, V. K., Sakai, T., Pokatayev, V., Yang, K., Wu, J., Dobbs, N., & Yan, N. (2017). Trafficking-mediated STING degradation requires sorting to acidified Endolysosomes and can be targeted to enhance anti-tumor response. *Cell Reports*, *21*, 3234–3242. https://doi.org/10.1016/j.celrep.2017.11.061

Haag, S. M., Gulen, M. F., Reymond, L., Gibelin, A., Abrami, L., Decout, A., Heymann, M., van der Goot, F. G., Turcatti, G., Behrendt, R., & Ablasser, A. (2018). Targeting STING with covalent small-molecule inhibitors. *Nature*, *559*, 269–273. https://doi.org/10.1038/s41586-018-0287-8

Hansen, A. L., Buchan, G. J., Rühl, M., Mukai, K., Salvatore, S. R., Ogawa, E., Andersen, S. D., Iversen, M. B., Thielke, A. L., Gunderstofte, C., Motwani, M., Møller, C. T., Jakobsen, A. S., Fitzgerald, K. A., Roos, J., Lin, R., Maier, T. J., Goldbach-Mansky, R., Miner, C. A., … Holm, C. K. (2018). Nitro-fatty acids are formed in response to virus infection and are potent inhibitors of STING palmitoylation and signaling. *Proceedings of the National Academy of Sciences of the United States of America*, *115*, E7768–E7775. https://doi.org/10.1073/pnas.1806239115

Huang, R., Ning, Q., Zhao, J., Zhao, X., Zeng, L., Yi, Y., & Tang, S. (2022). Targeting STING for cancer immunotherapy: From mechanisms to translation. *International Immunopharmacology*, *113*, 109304. https://doi.org/10.1016/j.intimp.2022.109304

Ishikawa, H., & Barber, G. N. (2008). STING is an endoplasmic reticulum adaptor that facilitates innate immune signalling. *Nature*, *455*, 674–678. https://doi.org/10.1038/nature07317

Ishikawa, H., Ma, Z., & Barber, G. N. (2009). STING regulates intracellular DNA-mediated, type i interferon-dependent innate immunity. *Nature*, *461*, 788–792. https://doi.org/10.1038/nature08476

Johnson, V. E., Stewart, J. E., Begbie, F. D., Trojanowski, J. Q., Smith, D. H., & Stewart, W. (2013). Inflammation and white matter degeneration persist for years after a single traumatic brain injury. *Brain*, *136*, 28–42. https://doi.org/10.1093/brain/aws322

Karve, I. P., Zhang, M., Habgood, M., Frugier, T., Brody, K. M., Sashindranath, M., Ek, C. J., Chappaz, S., Kile, B. T., Wright, D., & Wang, H. (2016). Ablation of type-1 IFN signaling in hematopoietic cells confers protection following traumatic brain injury. *ENeuro*, *3*, 89–93.

Khellaf, A., Khan, D. Z., & Helmy, A. (2019). Recent advances in traumatic brain injury. *Journal of Neurology*, *266*, 2878–2889. https://doi.org/10.1007/s00415-019-09541-4

Knoblach, S. M., Fan, L., & Faden, A. I. (1999). Early neuronal expression of tumor necrosis factor-α after experimental brain injury contributes to neurological impairment. *Journal of Neuroimmunology*, *95*, 115–125. https://doi.org/10.1016/S0165-5728(98)00273-2

Kong, L., Li, W., Chang, E., Wang, W., Shen, N., Xu, X., Wang, X., Zhang, Y., Sun, W., Hu, W., & Xu, P. (2022). mtDNA-STING Axis mediates microglial polarization via IRF3/NF-κB signaling after ischemic stroke. *Frontiers in Immunology*, *13*, 1538.

Krizsan-Agbas, D., Winter, M. K., Eggimann, L. S., Meriwether, J., Berman, N. E., Smith, P. G., & McCarson, K. E. (2014). Gait analysis at multiple speeds reveals differential functional and structural outcomes in response to graded spinal cord injury. *Journal of Neurotrauma*, *31*(9), 846–856. https://doi.org/10.1089/neu.2013.3115

Lawrence, T., Helmy, A., Bouamra, O., Woodford, M., Lecky, F., & Hutchinson, P. J. (2016). Traumatic brain injury in England and Wales: Prospective audit of epidemiology, complications and standardised mortality. *BMJ Open*, *6*, 12197.

cLee, Y., Lee, S., Chang, S. C., & Lee, J. (2019). Significant roles of neuroinflammation in Parkinson's disease: Therapeutic targets for PD prevention. *Archives of Pharmacal Research*, *42*, 416–425. https://doi.org/10.1007/s12272-019-01133-0

Lilley, E., Stanford, S. C., Kendall, D. E., Alexander, S. P., Cirino, G., Docherty, J. R., George, C. H., Insel, P. A., Izzo, A. A., Ji, Y., Panettieri, R. A., Sobey, C. G., Stefanska, B., Stephens, G., Teixeira, M., & Ahluwalia, A. (2020). ARRIVE 2.0 and the British Journal of Pharmacology: Updated guidance for 2020. *British Journal of Pharmacology*, *177*, 3611–3616. https://bpspubs.onlinelibrary.wiley.com/doi/full/10.1111/bph.15178

Loane, D. J., Kumar, A., Stoica, B. A., Cabatbat, R., & Faden, A. I. (2014). Progressive neurodegeneration after experimental brain trauma: Association with chronic microglial activation. *Journal of Neuropathology and Experimental Neurology*, *73*, 14–29. https://doi.org/10.1097/NEN.0000000000000021

Mathur, V., Burai, R., Vest, R. T., Bonanno, L. N., Lehallier, B., Zardeneta, M., Mistry, K. N., do, D., Marsh, S. E., Abud, E. M., Blurton-Jones, M., Li, L., Lashuel, H. A., & Wyss-Coray, T. (2017). Activation of the STING-dependent type I interferon response reduces microglial reactivity and neuroinflammation. *Neuron*, *96*, 1290–1302.e6. https://doi.org/10.1016/j.neuron.2017.11.032

McConeghy, K. W., Hatton, J., Hughes, L., & Cook, A. M. (2012). A review of neuroprotection pharmacology and therapies in patients with acute traumatic brain injury. *CNS Drugs*, *26*, 613–636. https://doi.org/10.2165/11634020-000000000-00000

Minter, M. R., Moore, Z., Zhang, M., Brody, K. M., Jones, N. C., Shultz, S. R., Taylor, J. M., & Crack, P. J. (2016). Deletion of the type-1 interferon receptor in APPSWE/PS1ΔE9 mice preserves cognitive function and alters glial phenotype. *Acta Neuropathologica Communications*, *4*, 72. https://doi.org/10.1186/s40478-016-0341-4

Moore, Z., Mobilio, F., Walker, F. R., Taylor, J. M., & Crack, P. J. (2020). Abrogation of type-I interferon signalling alters the microglial response to Abeta1-42. *Scientific Reports*, *10*, 3153. https://doi.org/10.1038/s41598-020-59917-0

Nazmi, A., Field, R. H., Griffin, E. W., Haugh, O., Hennessy, E., Cox, D., Reis, R., Tortorelli, L., Murray, C. L., Lopez-Rodriguez, A. B., Jin, L., Lavelle, E. C., Dunne, A., & Cunningham, C. (2019). Chronic neurodegeneration induces type I interferon synthesis via STING, shaping microglial phenotype and accelerating disease progression. *Glia*, *67*, 1254–1276. https://doi.org/10.1002/glia.23592

Neumann, M., Wang, Y., Kim, S., Hong, S. M., Jeng, L., Bilgen, M., & Liu, J. (2009). Assessing gait impairment following experimental traumatic brain injury in mice. *Journal of Neuroscience Methods*, *176*(1), 34–44. https://doi.org/10.1016/j.jneumeth.2008.08.026

Osier, N. D., & Dixon, C. E. (2016). The controlled cortical impact model: Applications,considerations for researchers, and future directions. *Frontiers in Neurology*, *7*. https://doi.org/10.3389/fneur.2016.00134

Peng, Y., Zhuang, J., Ying, G., Zeng, H., Zhou, H., Cao, Y., Chen, H., Xu, C., Fu, X., Xu, H., Li, J., Cao, S., Chen, J., Gu, C., Yan, F., & Chen, G. (2020). Stimulator of IFN genes mediates neuroinflammatory injury by suppressing AMPK signal in experimental subarachnoid hemorrhage. *Journal of Neuroinflammation*, *17*, 165. https://doi.org/10.1186/s12974-020-01830-4

Percie du Sert, N., Hurst, V., Ahluwalia, A., Alam, S., Avey, M. T., Baker, M., Browne, W. J., Clark, A., Cuthill, I. C., Dirnagl, U., Emerson, M., Garner, P., Holgate, S. T., Howells, D. W., Karp, N. A., Lazic, S. E., Lidster, K., MacCallum, C. J., Macleod, M., … Würbel, H. (2020). The ARRIVE guidelines 2.0: Updated guidelines for reporting animal research. *British Journal of Pharmacology*, *177*, 3617–3624. https://doi.org/10.1111/bph.15193

Rorden, C., & Brett, M. (2000). Stereotaxic display of brain lesions. *Behavioural Neurology*, *12*, 191–200. https://doi.org/10.1155/2000/421719

Sashindranath, M., Daglas, M., & Medcalf, R. L. (2015). Evaluation of gait impairment in mice subjected to craniotomy and traumatic brain injury. *Behavioural Brain Research*, *286*, 33–38. https://doi.org/10.1016/j.bbr.2015.02.038

Schmittgen, T. D., & Livak, K. J. (2008). Analyzing real-time PCR data by the comparative C(T) method. *Nature Protocols*, *3*, 1101–1108. https://doi.org/10.1038/nprot.2008.73

Sen, T., Saha, P., Gupta, R., Foley, L. M., Jiang, T., Abakumova, O. S., Hitchens, T. K., & Sen, N. (2020). Aberrant ER stress induced neuronal-IFNbeta elicits white matter injury due to microglial activation and T-cell infiltration after TBI. *The Journal of Neuroscience*, *40*, 424–446. https://doi.org/10.1523/JNEUROSCI.0718-19.2019

Shang, G., Zhang, C., Chen, Z. J., Bai, X., & Zhang, X. (2019). Cryo-EM structures of STING reveal its mechanism of activation by cyclic GMP–AMP. *Nature*, *567*, 389–393. https://doi.org/10.1038/s41586-019-0998-5

Sheridan, C. (2019). Drug developers switch gears to inhibit STING. *Nature Biotechnology*, *37*, 199–201. https://doi.org/10.1038/s41587-019-0060-z

Simon, D. W., McGeachy, M. J., Bayır, H., Clark, R. S. B., Loane, D. J., & Kochanek, P. M. (2017). The far-reaching scope of neuroinflammation after traumatic brain injury. *Nature Reviews. Neurology*, *13*, 171–191. https://doi.org/10.1038/nrneurol.2017.13

Sliter, D. A., Martinez, J., Hao, L., Chen, X., Sun, N., Fischer, T. D., Burman, J. L., Li, Y., Zhang, Z., Narendra, D. P., Cai, H., Borsche, M., Klein, C., & Youle, R. J. (2018). Parkin and PINK1 mitigate STING-induced inflammation. *Nature*, *561*, 258–262. https://doi.org/10.1038/s41586-018-0448-9

Sun, J., Zhou, Y., Xu, B. Y., Li, J. Y., Zhang, L. Q., Li, D. Y., Zhang, S., Wu, J. Y., Gao, S. J., Ye, D. W., & Mei, W. (2022). STING/NF-κB/IL-6-mediated inflammation in microglia contributes to spared nerve injury (SNI)-induced pain initiation. *Journal of Neuroimmune Pharmacology*, *17*, 453–469. https://doi.org/10.1007/s11481-021-10031-6

Sun, L., Wu, J., Du, F., Chen, X., & Chen, Z. J. (2013). Cyclic GMP-AMP synthase is a cytosolic DNA sensor that activates the type I interferon pathway. *Science*, *1979*(3-4), 786–791.

Tanaka, Y., & Chen, Z. J. (2012). STING specifies IRF3 phosphorylation by TBK1 in the cytosolic DNA signaling pathway. *Science Signaling*, *5*, ra20.

Vaughn, M. G., Salas-Wright, C. P., John, R., Holzer, K. J., Qian, Z., & Veeh, C. (2019). Traumatic brain injury and psychiatric co-morbidity in the United States. *The Psychiatric Quarterly*, *90*, 151–158. https://doi.org/10.1007/s11126-018-9617-0

Wangler, L. M., Bray, C. E., Packer, J. M., Tapp, Z. M., Davis, A. C., O'Neil, S. M., Baetz, K., Ouviña, M., Witzel, M., & Godbout, J. P. (2022). Amplified gliosis and interferon-associated inflammation in the aging brain following diffuse traumatic brain injury. *Journal of Neuroscience*, *42*, 9082–9096. https://doi.org/10.1523/JNEUROSCI.1377-22.2022

Witcher, K. G., Bray, C. E., Chunchai, T., Zhao, F., O'Neil, S. M., Gordillo, A. J., Campbell, W. A., McKim, D. B., Liu, X., Dziabis, J. E., Quan, N., Eiferman, D. S., Fischer, A. J., Kokiko-Cochran, O. N., Askwith, C., & Godbout, J. P. (2021). Traumatic brain injury causes chronic cortical inflammation and neuronal dysfunction mediated by microglia. *Journal of Neuroscience*, *41*, 1597–1616. https://doi.org/10.1523/JNEUROSCI.2469-20.2020

Wu, J., Dobbs, N., Yang, K., & Yan, N. (2020). Interferon-independent activities of mammalian STING mediate antiviral response and tumor immune evasion. *Immunity*, *53*, 115–126.e5. https://doi.org/10.1016/j.immuni.2020.06.009

Yu, C. H., Davidson, S., Harapas, C. R., Hilton, J. B., Mlodzianoski, M. J., Laohamonthonkul, P., Louis, C., Low, R. R. J., Moecking, J., de Nardo, D., Balka, K. R., Calleja, D. J., Moghaddas, F., Ni, E., McLean, C. A., Samson, A. L., Tyebji, S., Tonkin, C. J., Bye, C. R., … Masters, S. L. (2020). TDP-43 triggers mitochondrial DNA release via mPTP to activate cGAS/STING in ALS. *Cell*, *183*, 636–649.e18. https://doi.org/10.1016/j.cell.2020.09.020

Yu, Z., Fu, R., Li, Y., Zhao, D. Y., Jiang, H., & Han, D. (2023). The STING inhibitor C-176 attenuates osteoclast-related osteolytic diseases by inhibiting osteoclast differentiation. *The FASEB Journal*, *37*, e22867. https://doi.org/10.1096/fj.202201600R

Zhang, C., Shang, G., Gui, X., Zhang, X., Bai, X., & Chen, Z. J. (2019). Structural basis of STING binding with and phosphorylation by TBK1. *Nature*, *567*, 394–398. https://doi.org/10.1038/s41586-019-1000-2

Zhang, L. M., Xin, Y., Wu, Z. Y., Song, R. X., Miao, H. T., Zheng, W. C., Li, Y., Zhang, D. X., & Zhao, X. C. (2022). STING mediates neuroinflammatory response by activating NLRP3-related pyroptosis in severe traumatic brain injury. *Journal of Neurochemistry*, *162*, 444–462. https://doi.org/10.1111/jnc.15678

Zhang, M., Downes, C. E., Wong, C. H. Y., Brody, K. M., Guio-Agulair, P. L., Gould, J., Ates, R., Hertzog, P. J., Taylor, J. M., & Crack, P. J. (2017). Type-I interferon signalling through IFNAR1 plays a deleterious role in the outcome after stroke. *Neurochemistry International*, *108*, 472–480. https://doi.org/10.1016/j.neuint.2017.06.009

SUPPORTING INFORMATION

Additional supporting information can be found online in the Supporting Information section at the end of this article.

How to cite this article: Fryer, A. L., Abdullah, A., Mobilio, F., Jobling, A., Moore, Z., de Veer, M., Zheng, G., Wong, B. X., Taylor, J. M., & Crack, P. J. (2024). Pharmacological inhibition of STING reduces neuroinflammation-mediated damage post-traumatic brain injury. *British Journal of Pharmacology*, *181*(17), 3118–3135. https://doi.org/10.1111/bph.16347